Matematisk-fysiske Skrifter
udgivet af
Det Kongelige Danske Videnskabernes Selskab
Bind **2**, nr. 3

Mat. Fys. Skr. Dan. Vid. Selsk. **2**, no. 3 (1962)

SHELL MODEL CALCULATIONS OF ALPHA DECAY RATES OF EVEN-EVEN SPHEROIDAL NUCLEI

BY

H. J. MANG AND J. O. RASMUSSEN

København 1962
i kommission hos Ejnar Munksgaard

DET KONGELIGE DANSKE VIDENSKABERNES SELSKAB udgiver følgende publikationsrækker:

THE ROYAL DANISH ACADEMY OF SCIENCES AND LETTERS *issues the following series of publications:*

	Bibliographical Abbreviation
Oversigt over Selskabets Virksomhed (8°) *(Annual in Danish)*	Overs. Dan. Vid. Selsk.
Historisk-filosofiske Meddelelser (8°) Historisk-filosofiske Skrifter (4°) *(History, Philology, Philosophy, Archeology, Art History)*	Hist. Filos. Medd. Dan. Vid. Selsk. Hist. Filos. Skr. Dan. Vid. Selsk.
Matematisk-fysiske Meddelelser (8°) Matematisk-fysiske Skrifter (4°) *(Mathematics, Physics, Chemistry, Astronomy, Geology)*	Mat. Fys. Medd. Dan. Vid. Selsk. Mat. Fys. Skr. Dan. Vid. Selsk.
Biologiske Meddelelser (8°) Biologiske Skrifter (4°) *(Botany, Zoology, General Biology)*	Biol. Medd. Dan. Vid. Selsk. Biol. Skr. Dan. Vid. Selsk.

Selskabets sekretariat og postadresse: Dantes Plads 5, København V.

The address of the secretariate of the Academy is:

Det Kongelige Danske Videnskabernes Selskab,
Dantes Plads 5, København V, Denmark.

Selskabets kommissionær: EJNAR MUNKSGAARD's Forlag, Nørregade 6, København K.

The publications are sold by the agent of the Academy:

EJNAR MUNKSGAARD, *Publishers,*
6 Nörregade, København K, Denmark.

Matematisk-fysiske Skrifter
udgivet af
Det Kongelige Danske Videnskabernes Selskab
Bind **2,** nr. 3

Mat. Fys. Skr. Dan. Vid. Selsk. **2,** no. 3 (1962)

SHELL MODEL CALCULATIONS OF ALPHA DECAY RATES OF EVEN-EVEN SPHEROIDAL NUCLEI

BY

H. J. MANG AND J. O. RASMUSSEN

København 1962
i kommission hos Ejnar Munksgaard

CONTENTS

Synopsis

The formulation of the alpha decay rate theory based on the independent-particle shell model wave functions, which has earlier been successfully applied to spherical nuclei, is here extended to apply to spheroidally deformed nuclei. This method essentially projects out of the shell model wave function of the most lightly bound neutrons and protons a finite-sized Gaussian, singlet-spin alpha-particle internal wave function, resulting in a wave function in the center-of-mass coordinate of the alpha cluster. This wave function serves to fix the boundary condition on the nuclear surface for the irregular type Coulomb wave solution through the anisotropic barrier. The independent-particle formulation is generalized to include correlation effects arising from the pairing interaction.

Numerical calculations of relative alpha intensities to rotational states of several even nuclei of elements 92–100 are carried out using Nilsson's numerical wave functions. The theoretical results nicely show the essential features of the relative intensity patterns, although the theoretical intensity of the decay to the first excited 2+ state is too high.

The absolute transition probability calculated for Cm^{242} is about a factor of 60 too low assuming IGO's optical model potential for the barrier, but the factor is extremely sensitive to this latter assumption.

The essential role of the configuration mixing induced by the pairing force in smoothing the decay rate trends from nucleus to nucleus and in giving a large enhancement of the absolute rate is pointed out in the discussion.

PRINTED IN DENMARK
BIANCO LUNOS BOGTRYKKERI A/S

Introduction

For some time it has been realized that there is a close connection between α-decay rates and the shell-model orbitals of the more lightly bound nucleons. Formulations of the problem have been made (MANG, 1957, 1959; BRUSSAARD and TOLHOEK, 1958) and quite a number of numerical calculations for spherical nuclei near doubly magic Pb^{208} have been carried out and compared with experiment (MANG, 1960).

There are extensive data on α-decay of spheroidally deformed nuclei, and the classification of nucleon states of odd-mass nuclei according to the Nilsson scheme (1955) has been carried out rather satisfactorily throughout the region of heavy deformed nuclei ($A \geq 229$) (MOTTELSON and NILSSON, 1959; STEPHENS, ASARO, and PERLMAN, 1959).

Despite the formidable computational difficulties involved, it appeared worth while to make an attempt at applying MANG's shell model formulation of α-decay to the spheroidal nuclear region, using the IBM-709 computer at the Lawrence Radiation Laboratory.

It has long appeared probable that α-decay to the ground rotational band of even-even nuclei involves an averaging of participation of many nucleon orbitals near the Fermi surface, since reduced widths and hindrance factors vary smoothly with nucleon numbers. From the outset it was clear that a meaningful calculation for even nuclei must involve repeated calculations of the contribution of various Nilsson orbital combinations followed by a weighted averaging process, weighting combinations according to the probability that a given orbital is occupied in the parent and vacant in the daughter. The Belyaev pairing interaction method (BELYAEV, 1959) was chosen, and we have drawn heavily on the analysis of NILSSON and PRIOR (1961) for numerical values of the energy gap parameter Δ as well as best values of the quadrupole deformation for given nuclei.

After a theoretical calculation of α-wave amplitudes in the region of the nuclear surface it was necessary to treat their propagation through the anisotropic barrier. The matrix method of FRÖMAN (1957) was used with certain important modifications which bring better agreement with the numerical work of RASMUSSEN and HANSEN (1958) on Cm^{242}. Preliminary results of the calculations herein described have been given previously in a brief report (MANG and RASMUSSEN, 1961).

I. Basic Formulas for the Decay Constant

Slightly generalizing a method (Mang, 1957, 1959, 1960) which has been described earlier, we obtain expressions for the asymptotic form of the total wave function of the α-decaying system* (Casimir, 1934) and for the decay constant

$$\left.\begin{aligned} \Psi_{R\to\infty} &\to \sum_{\sigma} \left[\left(\frac{N}{2}\right)\left(\frac{Z}{2}\right)\right]^{1/2} \frac{\hbar^2}{2M} \int dS\, d\xi_\alpha\, d\xi_K \left[\overset{*}{\Phi}{}_J^{M K_0 q} \overset{\leftrightarrow}{\frac{\partial}{\partial n}} \Psi^M_{\sigma E J} \right]_{E=E_0} \Psi^{+M}_{\sigma E J} \\ \lambda &= \frac{2\pi}{\hbar}\left(\frac{N}{2}\right)\left(\frac{Z}{2}\right) \sum_{\sigma} \left| \frac{\hbar^2}{2M} \int dS\, d\xi_\alpha\, d\xi_K \left[\overset{*}{\Phi}{}_J^{M K_0 q} \overset{\leftrightarrow}{\frac{\partial}{\partial n}} \Psi^M_{\sigma E J} \right]_{E=E_0} \right|^2, \end{aligned}\right\} \quad \text{(I. 1)}$$

where

$$\Psi^{+M}_{\sigma E J} = \text{outgoing part of } \Psi^M_{\sigma E J}.$$

In (I. 1), $\Phi_J^{M K_0 q}$ is the wave function of the parent nucleus and E_0 is its total energy. $\Psi^M_{\sigma E J}$ describes the final state α-particle plus daughter nucleus. The index σ is a shorthand notation for all quantum numbers specifying the final state, except the total energy and the angular momentum J, M. The coordinates ξ_α and ξ_K are internal coordinates of the α-particle and daughter nucleus. The closed surface S in the space of the vector R, the distance between α-particle and daughter nucleus, is so chosen that outside S the interaction between an α-particle and the daughter nucleus may be described by a potential $V(R)$, whereas inside S an individual nucleon, shell model type representation should be valid. As will be seen later, it is of essential importance that the pairing force effects be added to the Nilsson model.

As will be discussed again later, there is uncertainty as to the effective potential experienced by the α-particle close to the nucleus. We suppose the outer tail of the effective nuclear potential to be not too different from the real part of Igo's optical model potential (Igo, 1959) derived from α-scattering. Of course, by introducing an anisotropic nuclear potential we have gone beyond the Igo potential and introduced a mechanism for exchange of energy between the α-particle and the rotational degrees of freedom of the nucleus. The region of validity of the outer representation (α-particle + daughter nucleus) can, in principle, be brought inward further and further by introduction of additional couplings between α-particle and internal degrees of freedom of the daughter nucleus. Likewise, the region of validity of the inner representation (individual nucleon product wave function) can be extended outward by improvements in the Hamiltonian, especially with regard to representing the tendency toward nucleon clustering, expected to be most important in the surface region (cf. Wilkinson, 1961). The addition of the pairing interaction is an important improvement in this direction, but there is not yet a clear way to include the specific neutron-proton cor-

* The symbol $\left[\overset{*}{\Phi} \overset{\leftrightarrow}{\frac{\partial}{\partial n}} \Psi\right]$ is defined as $\overset{*}{\Phi} \frac{\partial}{\partial n} \Psi - \frac{\partial}{\partial n} \overset{*}{\Phi} \Psi$, where $\frac{\partial}{\partial n}$ is the derivative normal to the surface S.

relations expected from the special stability of the α-cluster. The leveling off of the Nilsson oscillator potential in the surface region is another needed improvement, for the oscillator potential attenuates the wave function much too drastically in the outermost region of main interest here. If, by such improvements to the Hamiltonians in both the inner and the outer region, the regions can be made to overlap, then the connection surface may be chosen anywhere within the region of overlap, and the theoretical decay constant will be independent of the exact choice. Of course, neither Hamiltonian can ever be perfect and the connecting surface will always be located as a compromise where both inner and outer descriptions are still fairly good. It would seem that the best choice of S will be along a surface of constant nuclear density. Serious problems arise in carrying the external α-wave solutions inward through an inner classical turning point with an anisotropic potential. Thus, one is compelled to locate the connection surface within the α-barrier. We shall choose it along a surface of constant nuclear density somewhat more than 1×10^{-13} cm beyond the effective charge radius $1.2\times10^{-13}\,A^{1/3}$ cm.

In a next step of the development we shall define the wave functions which enter into Eq. (I. 1). The wave function $\Phi_J^{MK_0q}$ will be a solution of the strong-coupling Hamiltonian of BOHR and MOTTELSON (1953)

$$\left.\begin{aligned} \{H_{\mathrm{rot}}(\Theta_i)+H_{\mathrm{intrinsic}}-E_0\}\,\Phi_J^{MK_0q}&=0\\ \Phi_J^{MK_0q}&=\sqrt{\frac{2J+1}{16\pi^2}}\{D^J_{MK_0}X_{K_0}+(-1)^{J-q-K_0}D^J_{M-K_0}X_{-K_0}\}. \end{aligned}\right\} \qquad \text{(I. 2)}$$

The functions $D^J_{MK_0}$, the eigenfunctions to the symmetric top, are eigenfunctions of the rotational Hamiltonian H_{rot}. The Eulerian angles Θ_i connect the "body-fixed" nuclear coordinate system with a "space-fixed" frame of reference. The wave functions X_{K_0} are eigenfunctions of the intrinsic Hamiltonian $H_{\mathrm{intrinsic}}$. We shall use NILSSON's model Hamiltonian with a pairing interaction included to approximate H_{intr}. The phase factor $(-1)^{J-q-K_0}$, where $(-1)^q$ is the parity of the state, differs somewhat from the one given by BOHR and MOTTELSON, but this is due to a different phase choice for X_{-K_0} which will later turn out to be convenient. The wave functions $\Psi^M_{\sigma EJ}$ describing the final state of the system are solutions of

$$\left\{H_{\mathrm{rot}}+H_{\mathrm{intr}}(\mathrm{daughter})+H_\alpha(\xi_\alpha)-\frac{\hbar^2}{2M}\Delta_{\mathrm{R}}+V(R,\,\Theta_i)-E\right\}\Psi^M_{\sigma EJ}=0. \qquad \text{(I. 3)}$$

The Eulerian angles Θ_i have been inserted in $V(R,\,\Theta_i)$ to exhibit the dependence of the anisotropic potential on the nuclear orientation. It should be pointed out that the Eulerian angles Θ_i are included in the coordinates ξ_K of Eq. (I. 1).

The $\Psi^M_{\sigma EM}$ are regular everywhere (standing-wave solutions) and *normalized* as follows:

$$\int d\xi_\alpha \, d\xi_K \, d^3R \, \overset{*}{\Psi}{}^{M'}_{\sigma' E' J'} \, \Psi^{M}_{\sigma E J} = \delta_{\sigma\sigma'} \, \delta_{MM'} \, \delta_{JJ'} \, \delta(E - E'), \tag{I. 4}$$

where E is the total energy of the system.

We shall also need the irregular (standing-wave) solutions of (I. 3), irregular as functions of R. They will be denoted by $\Phi^{M}_{\sigma E J}$ and we note the important relation which normalizes these functions

$$\int dS \, d\xi_\alpha \, d\xi_K \, \overset{*}{\Psi}{}^{M}_{\sigma E J} \overleftrightarrow{\frac{\partial}{\partial n}} \Phi^{M}_{\sigma' E J} = \frac{2M}{\pi \hbar^2} \, \delta_{\sigma\sigma'} \tag{I. 5}$$

where S may be any closed surface around the origin, in particular the connection surface mentioned earlier.

At this point some words should be said about the terms "regular and irregular solutions". To define such solutions the potential $V(R)$ must be defined throughout the nuclear volume, a procedure which seems to be somewhat arbitrary. But, because of the small penetrability, the potential inside the nucleus may be changed somewhat without changing the solutions in the barrier region. It is well known from the simple case of a central potential when the W-K-B approximation is valid that the regular solution is the one which increases in the barrier region with increasing distance R and is linearly independent of the irregular solution which continually decreases throughout the barrier and that this behaviour is rather independent of the potential inside the nucleus. In such a sense the terms irregular and regular will be used from now on.

We write $\Phi^{M}_{\sigma E J}$ in general as follows:

$$\Phi^{PKM}_{\sigma E J} = \chi_\alpha \sqrt{\frac{2M}{\pi \hbar^2 k_0}} \sum_{l' m'} a^{\sigma}_{l' m'} \sum_{lm} \frac{g^{l' m'}_{lm}(R)}{R} \varphi^{PKM}_{mlJ}, \tag{I. 6}$$

where

$$\varphi^{PKM}_{mlJ} = \sqrt{\frac{2J+1}{16\pi^2}} \left\{ D^{J}_{MK+m} \, X_K \, Y^{m}_{l}(\vartheta' \varphi') + (-1)^{J-L-P-K} \, D^{J}_{M-K-m} \, X_{-K} \, Y^{-m}_{l}(\vartheta' \varphi') \right\},$$

$\frac{\hbar^2}{2M} k_0^2 = \varepsilon_{\max}$, $\varepsilon_{\max}$ being the maximum kinetic energy of an α-particle involved in the process. In (I. 6) χ_α is the internal α-particle wave function, X_K the intrinsic wave function of the daughter nucleus, and $(-1)^P$ its parity. The quantum numbers K and P were originally included in the set σ, but from now on it is convenient to exhibit the dependence of the wave function on them explicitly. The functions $g^{l' m'}_{lm}(R)$ constitute dimensionless components, indexed lm, of a set, indexed $l'm'$, of linearly independent solutions of the coupled α-wave equations.

$$\left\{-\frac{\hbar^2}{2M}\frac{d^2}{dR^2}+V(R)+\frac{\hbar^2}{2M}\frac{l(l+1)}{R^2}-\varepsilon\right\} g_{lm}^{l'm'}(R) = -\sum_{l''} V_{ll''}^{m}(R)\, g_{l''m}^{l'm'}(R) - \sum_{m''} A_{m}^{m''}(KlJ)\, g_{lm''}^{l'm'}(R), \tag{I. 7}$$

where

$$A_{m}^{m''}(KlJ) = \sum_{j} E_{\mathrm{rot}}(jK)(-1)^{m-m''} C(Jlj;\, K+m-m)\, C(Jlj;\, K+m''-m''),$$

reducing for even-even nuclear decay to $\frac{\hbar^2}{2\Im} l(l+1)$

$$V_{ll''}^{m} = \int \overset{*}{Y}_{l}^{m}\, V(R, \vartheta', \varphi')\, Y_{l''}^{m}\, d\Omega'.$$

The potential $V(R\vartheta'\varphi')$ is the non-central part of $V(R\Theta_i)$. An analogous expansion to (I. 6) could be written down for the regular functions $\Psi_{\sigma EJ}^{PKM}$, but it will turn out later that we do not need explicit expressions for regular solutions. The boundary conditions determining the various solutions $(l'm')$ are imposed along a connection surface of cylindrical symmetry $R_s(\vartheta')$. Firstly, the wave amplitude of solution $(l'm')$ should vary as $Y_l^{m'}(\vartheta'\varphi')$ along the surface $R_s(\vartheta')$. Secondly, the first derivative normal to the surface is to be fixed such that the solution should not go into exponentially increasing behaviour anywhere within the barrier. This gives exactly the irregular solution, as has been explained earlier.

Formally we may write the first condition as

$$\sum_{lm} g_{lm}^{l'm'}(R_s(\vartheta'))\, \varphi_{mlJ}^{PKM} = \varphi_{m'l'J}^{PKM}.$$

If the connection surface were a sphere, this normalization would mean a value of unity for diagonal elements $g_{l'm'}^{l'm'}(R_s)$ and zero for off-diagonal. The condition on the derivatives will, for practical purposes, be satisfied by constructing solutions in the barrier region from linear combinations of irregular Coulomb functions or decreasing W-K-B solutions.

The expansion coefficients $a_{l'm'}^{\sigma}$ are free to be determined by the boundary conditions at the nuclear surface subject to the restriction that the normalization conditions (I. 4) and (I. 5) are fulfilled.

We shall now discuss the boundary condition which actually will be imposed on our solutions $\Phi_{\sigma EJ}^{PKM}$. If the inner and outer region Hamiltonians are both correct at the connection surface S, as has been assumed in the context of Eq. (I. 1), then there are particular irregular solutions $\Phi_{E_0K_0-KJ}^{PKM}$ and $\Phi_{E_0K_0+KJ}^{PKM}$ for any quantum number K, characterizing a rotational band in the daughter nucleus, and these solutions have the following properties:

$$\left.\begin{aligned}
\Phi^{PKM}_{E_0 K_0 - KJ} &\overset{\text{at } S}{=} \chi_\alpha \sqrt{\frac{2M}{\pi\hbar^2 k_0}} \sum_{l'} \frac{a_{l' K_0 - K}}{R_s} \varphi^{PKM}_{K_0 - K l' J} \\
&\overset{\text{at } S}{=} C_{K_0 - K} \chi_\alpha \sqrt{\frac{2M}{\pi\hbar^2 k_0}} \sum_{L} R_s^{-3/2} G_{L K_0 - K}(R_s) \varphi^{PKM}_{K_0 - K LJ} \\
\Phi^{PKM}_{E_0 K_0 + KJ} &\overset{\text{at } S}{=} \chi_\alpha \sqrt{\frac{2M}{\pi\hbar^2 k_0}} \sum_{l'} \frac{a_{l' K_0 + K}}{R_s} \varphi^{PKM}_{-K_0 - K l' J} \\
&\overset{\text{at } S}{=} C_{K_0 + K} \chi_\alpha \sqrt{\frac{2M}{\pi\hbar^2 k_0}} \sum_{L} R_s^{-3/2} G_{L K_0 + K}(R_s) \varphi^{PKM}_{-K_0 - K LJ}
\end{aligned}\right\} \quad \text{(I. 8)}$$

where

$$\frac{a_{l' m'}}{C_{m'}} = \sum_{L} \int \overset{*}{Y}{}^{m'}_{l'}(\vartheta' \varphi') R_s^{-1/2} G_{L m'}(R_s) Y^{m'}_{L}(\vartheta' \varphi') \, d\Omega'$$

$$G_{L K_0 - K}(R) = R^{3/2} \left[\binom{N}{2}\binom{Z}{2}\right]^{1/2} \int \overset{*}{X}_{K_0} \chi_\alpha X_K \, Y_L^{K_0 - K} \, d\xi_\alpha \, d\xi_K \, d\Omega'$$

$$G_{L K_0 + K}(R) = R^{3/2} \left[\binom{N}{2}\binom{Z}{2}\right]^{1/2} (-1)^P \int \overset{*}{X}_{K_0} \chi_\alpha X_{-K} \, Y_L^{K_0 + K} \, d\xi_\alpha \, d\xi_K \, d\Omega'.$$

Analogous relations to (I. 8) are valid for the derivatives normal to S. The constants $C_{K_0 - K}$, $C_{K_0 + K}$ (of dimension $R^{1/2}$) are introduced so that the $\Phi^{PKM}_{E_0 mJ}$ are properly normalized according to (I. 5) and (I. 4). The factor $\left[\binom{N}{2}\binom{Z}{2}\right]^{1/2}$ in the definition of $G_{Lm}(R)$ has been introduced so that G_{Lm} is the probability amplitude for finding an α-particle with angular momentum L at a radial distance R. G_{Lm} is defined in dimensionless fashion, so the identification as an effective one-dimensional internal radial wave function requires it to be divided by $R^{1/2}$. The boundary condition (I. 8) is the usual one made in resonance theory when dealing with a quasi-stationary state (THOMAS, 1954). The solution in the inner region joins smoothly to the irregular solution in the outer region. In the case of a purely central Coulomb potential this would be the well-known irregular Coulomb wave function. If, later on, the functions G_{Lm} calculated from model wave functions should not fulfill exactly the boundary condition (I. 8), this will be due to the fact that our model is not accurate enough. One of the improvements mentioned in connection with the definition of the surface should then be made. Actual calculations for spherical nuclei (ZEH and MANG, 1961) show that in the nuclear surface region the logarithmic derivative of G_{Lm} deviates by less than $20\,\%$ from that of the irregular Coulomb function.

The two particular solutions which have been selected by Eq. (I. 8) may now be considered as the first two of a whole set which of course must fulfill the condition (I. 5).

If we now consider that part of the parent wave function $\Phi_J^{MK_0q}$ that is proportional to χ_α (i.e. contains an α-particle), it may be expanded at the nuclear surface in terms of functions $\Phi_{E_0mJ}^{PKM}$. Therefore, the sum on σ in (I. 1) contains only a sum on K and for each K the two terms defined in (I. 8), and we get

$$\left.\begin{aligned}
&\left[\binom{N}{2}\binom{Z}{2}\right]^{1/2}\int\left[\overset{*}{\Phi}{}_J^{MK_0q}\overset{\leftrightarrow}{\frac{\partial}{\partial n}}\Psi_{E_0mJ}^{PKM}\right]dS\,d\xi_\alpha\,d\xi_K\\
&=\sqrt{\frac{\pi\hbar^2k_0}{2M}}\left\{\frac{\delta_{m,\,K_0-K}}{C_{K_0-K}}\int\left[\overset{*}{\Phi}{}_{E_0K_0-KJ}^{PKM}\overset{\leftrightarrow}{\frac{\partial}{\partial n}}\Psi_{E_0K_0-KJ}^{PKM}\right]dS\,d\xi_\alpha\,d\xi_K\right.\\
&\left.+\frac{\delta_{m,\,K_0+K}}{C_{K_0+K}}(-1)^{J-q-P-K}\int\left[\overset{*}{\Phi}{}_{E_0K_0+KJ}^{PKM}\overset{\leftrightarrow}{\frac{\partial}{\partial n}}\Psi_{E_0K_0+KJ}^{PKM}\right]dS\,d\xi_\alpha\,d\xi_K\right\}\\
&=\sqrt{\frac{2Mk_0}{\pi\hbar^2}}\left[\frac{\delta_{m,\,K_0-K}}{C_{K_0-K}}+\frac{(-1)^{J-q-P-K}\,\delta_{m,\,K_0+K}}{C_{K_0+K}}\right].
\end{aligned}\right\}\qquad\text{(I. 9)}$$

Eq. (I. 9) is strictly correct as long as the projection of the angular momentum on the nuclear symmetry axis is a constant of motion or, in other words, as long as K_0 and K are good quantum numbers. If we allow for Coriolis mixing of rotational bands, for instance, then (I. 9) has to be slightly generalized.

It is now easy to construct the asymptotic wave function using (I. 9).

$$\Psi_{R\to\infty}\sqrt{\frac{\pi\hbar^2k_0}{2M}}\sum_{KP}\left\{\frac{1}{C_{K_0-K}}\Psi_{E_0K_0-KJ}^{+\,PKM}+\frac{(-1)^{J-q-P-K}}{C_{K_0+K}}\Psi_{E_0K_0+KJ}^{+\,PKM}\right\}.\qquad\text{(I. 10)}$$

Of course, we may use the outgoing part of $\Phi_{E_0K_0-KJ}^{PKM}$ and $\Phi_{E_0K_0+KJ}^{PKM}$ as well, and indeed we shall make use of this possibility. We now consider the asymptotic behaviour of $\Phi_{E_0m'J}^{+\,PKM}$.

$$\Phi_{E_0m'J}^{+\,KPM}{}_{R\to\infty}\chi_\alpha\sqrt{\frac{2M}{\pi\hbar^2k_0}}\sum_{l'lm}a_{l'm'}\frac{g_{lm}^{+\,l'm'}(R)}{R}\varphi_{mlJ}^{PKM},\qquad\text{(I. 11)}$$

where

$$m'=\begin{cases}K_0-K\\K_0+K\end{cases}.$$

The $g_{lm}^{+\,l'm'}$ are the outgoing parts of the $g_{lm}^{l'm'}$ and follow from a solution of the α-wave equation. The meaning of the "matrix" $g_{lm}^{+\,l'm'}(R\to\infty)$ may be easily visualized: An α-particle which is formed in a state $l'm'$ at the nuclear surface may be scattered by the anisotropic potential into states lm at infinity.

After transforming the $Y_l^m(\vartheta'\varphi')$ which are contained in φ_{mlJ}^{PKM} to the space-fixed coordinate system we get

$$\left.\begin{aligned}\Phi^{+PKM}_{E_0 m' J} &= \sum_{l' l m} a_{l' m'} \frac{g^{+l' m'}_{lm}(R)}{R} \sum_{\nu} \sqrt{\frac{2j+1}{2J+1}}\, C(ljJ;\, mK) \\ &\times \sum_{\nu} C(ljJ;\, \nu M-\nu)\, Y^{\nu}_{l}(\vartheta\varphi) \sqrt{\frac{2j+1}{16\pi^2}} \left\{ D^{j}_{M-\nu K} X_K + (-1)^{j-P-K} D^{j}_{M-\nu-K} X_{-K} \right\}.\end{aligned}\right\} \tag{I. 12}$$

We easily recognize the sum on ν as a properly normalized wave function of an α-particle with angular momentum l coupled to a rotational state of the daughter nucleus with angular momentum j to give the total angular momentum J. The transition probability to such a state is exactly what we are interested in. We now define a matrix $B^{l'm'}_{lj}$ through

$$\sum_{m} g^{+l' m'}_{lm} \sqrt{\frac{2j+1}{2J+1}}\, C(ljJ;\, mK) = B^{l' m'}_{lj}\, e^{i(k_j R + \delta^{\text{COULOMB}}_{ljK})}, \tag{I. 13}$$

where $k_j = \sqrt{\frac{2M}{\hbar^2}\varepsilon_j}$, ε_j being the kinetic energy of the α-transition leading to the state j.

The matrix $B^{l'm'}_{lj}$ has essentially the same meaning as $g^{l'm'}_{lm}$, only the states labeled by lm have been replaced by states labeled by lj. These states are indeed the appropriate ones to use because they belong to a definite energy of the emitted α-particle. Finally, we arrive at a formula for the asymptotic wave function which contains the desired information.

$$\left.\begin{aligned}\Psi_{R\to\infty} &\to \sum_{ljK} \sqrt{\frac{2M}{\pi\hbar^2 k_j}} \frac{e^{i(k_j R + \delta^{\text{COULOMB}}_{ljK})}}{R} \chi_\alpha \\ &\sum_{\nu} C(ljJ;\, \nu M-\nu)\, Y^{\nu}_{l}(\vartheta,\varphi) \sqrt{\frac{2j+1}{16\pi^2}} \left\{ D^{j}_{M-\nu K} X_K \right. \\ &\left. + (-1)^{j-P-K} D^{j}_{M-\nu-K} X_{-K} \right\} \sum_{l'} \left[B^{l' K_0 - K}_{lj} \frac{a_{l' K_0 - K}}{C_{K_0 - K}} \right. \\ &\left. + (-1)^{J-L-K} B^{l' K_0 + K}_{lj} \frac{a_{l' K_0 + K}}{C_{K_0 + K}} \right] \sqrt{\frac{\hbar}{2\pi}} v_j,\end{aligned}\right\} \tag{I. 14}$$

where

$$v_j = \sqrt{\frac{2\varepsilon_j}{M}}.$$

Eq. (I. 14) gives the decomposition of the asymptotic wave function into definite final states ljK. It follows therefore from Eq. (I. 14) that the transition rate from a state of the parent labeled by JK_0q to a state jKp of the daughter via emission of an α-particle with angular momentum l equals

$$\lambda_{ljKP}^{JK_0q} = v_j \left| \sum_{l'L} \left[B_{lj}^{l'K_0-K} \int d\Omega' \overset{*}{Y}_{l'}^{K_0-K} \frac{G_{LK_0-K}(R_s)}{R_s^{1/2}} Y_L^{K_0-K} \right. \right.$$
$$\left. \left. + (-1)^{J-L-K} B_{lj}^{l'K_0+K} \int d\Omega' \overset{*}{Y}_{l'}^{K_0+K} \frac{G_{LK_0+K}(R_s)}{R_s^{1/2}} Y_L^{K_0+K} \right] \right|^2 . \qquad \text{(I. 15)}$$

Of course, the total decay constant is given by

$$\lambda = \sum_{ljKP} \lambda_{LJKP}^{JK_0q} = \sum_{KP} \left(\frac{1}{C_{K_0-K}^2} + \frac{1}{C_{K_0+K}^2} \right) \frac{2Mk_0}{\pi\hbar^2} . \qquad \text{(I. 16)}$$

The last equality follows from the fact that, according to (I. 5),

$$\int \overset{*}{\Phi}_{E_0 m' J}^{+PKM} \overleftrightarrow{\frac{\partial}{\partial n}} \Phi_{E_0 m'' J}^{+P''K''M} d\xi_\alpha \, d\xi_K \, dS = 2i \frac{2M}{\pi\hbar^2} \delta_{m'm''} \delta_{pp''} \delta_{KK''} \qquad \text{(I. 17)}$$

for any closed surface S around the origin. This relation, when applied to the asymptotic wave function, implies

$$\frac{2M}{\pi\hbar^2 k_0} \sum_{l'l''lj} k_j \overset{*}{a}_{l'm'} a_{l''m''} \overset{*}{B}_{lj}^{l'm'} B_{lj}^{l''m''} = \frac{2M}{\pi\hbar^2} \delta_{m'm''} . \qquad \text{(I. 18)}$$

From this equation (I. 18) the given result for the total decay constant follows immediately. On the other hand, this result could have been also obtained by inserting (I. 9) into (I. 1).

Before going on and treating special cases of (I. 16), we shall once more explain the meaning of the quantities appearing in the above equation. The function $R_s^{-1/2} G_{LM}(R_s)$ is, as already pointed out in connection with the boundary condition, the probability amplitude for forming an α-particle and a daughter nucleus out of the wave function of the parent. $R_s^{-1/2} G_{LM}$ depends essentially on the specific nuclear properties of the parent and daughter nucleus and is closely related to the reduced width of the transition (MANG, 1959a). On the other hand, $B_{lj}^{l'm'}$ depends mainly on gross nuclear properties as atomic weight A, charge Z, and quadrupole moment Q_0, the dependence on the angular momenta jKK_0 being nearly purely geometrical. In fact, $B_{lj}^{l'm'}$ tells us how an α-partial wave $l'm'$ of unit amplitude at the nuclear surface penetrates through the anisotropic potential barrier to give rise to an outgoing partial wave (lj) at large distances.

It may be useful here to give the expression for the matrix $B_{lj}^{l'm'}$ in the Fröman approximation (FRÖMAN, 1957) for the special case of even-even nuclear decay to the ground band of the daughter. In this case, $l = j$, $m' = 0$ and the coupled radial equations can be expressed like the standard Coulomb form as

$$\frac{d^2 u_l}{d\varrho^2} - \left[\frac{2\eta}{\varrho} - 1 + V_N(\varrho) + l(l+1)\left(\frac{1}{\varrho^2} + \varepsilon\right)\right] u_l = \frac{q}{\varrho^3} \sum_{l'} u_{l'} \langle Y_{l'}^0 \mid P_2 \mid Y_l^0 \rangle, \qquad \text{(I. 19)}$$

where $\eta = \dfrac{2Ze^2}{\hbar v_0}$ with v_0 the velocity of the ground alpha group,

$$\varepsilon = \frac{M}{\Im k_0}, \quad \varrho = k_0 R,$$

$q = \eta \dfrac{k_0^2 Q_0}{Z}$ with $\Im$ the nuclear moment of inertia, k_0 the ground alpha wave number, Q_0 the intrinsic quadrupole moment, $V_N(\varrho)$ is the short-range, attractive nuclear potential, and we have omitted coupling terms in $V_N(\varrho)$.

Then,

$$B_{ll}^{l'0}\,(\text{even-even}) = \frac{1}{G_l(\eta\varrho)}\, k_{ll'}(B), \qquad \text{(I. 20)}$$

where $G_l(\eta\varrho)$ is the irregular solution of the uncoupled equation for u_l with the right side set to zero. The reciprocal of the irregular function at the inner turning point is equivalent to the square root of the barrier penetrability factor.

We might mention that, inserting $\delta_{ll'}$ for $k_{ll'}$ and the WKB approximation for $G_l(\eta\varrho)$, we get results for spherical nuclei that have been derived earlier (Mang, 1960).

II. Formulas for Calculation of *G*-functions from the Shell Model

To calculate G_{LK_0-K} and G_{LK_0+K} explicitly we assume that the intrinsic properties of a deformed nucleus follow from a Hamiltonian of the type (Belyaev, 1958)

$$\left.\begin{aligned} H = &\sum_{\Omega_p} \varepsilon_{\Omega_p} \{a_{\Omega_p}^+ a_{\Omega_p} + a_{-\Omega_p}^+ a_{-\Omega_p}\} \\ &+ \sum_{\Omega_N} \varepsilon_{\Omega_N} \{a_{\Omega_N}^+ a_{\Omega_N} + a_{-\Omega_N}^+ a_{-\Omega_N}\} \\ &+ G_p \sum_{\Omega_p \Omega'_p} a_{\Omega_p}^+ a_{-\Omega_p}^+ a_{\Omega' p} a_{-\Omega' p} \\ &+ G_N \sum_{\Omega_N \Omega'_N} a_{\Omega_N}^+ a_{-\Omega_N}^+ a_{-\Omega' N} a_{-\Omega'}. \end{aligned}\right\} \qquad \text{(II. 1)}$$

The index p or N refers to protons and neutrons, respectively. The quantum number Ω labels the Nilsson orbits and the summation runs over all the orbits outside closed shells. The operator a_Ω^+ creates a particle in a state $\mid \varphi_\Omega \rangle$. The representation is that used by Nilsson (1955)

$$\varphi_\Omega = \sum_{l\Lambda} \alpha_{l\Lambda}\, \varphi_{nl}^{\Lambda}(\vec{r})\, \chi_{\pm 1/2}^{\Omega-\Lambda}. \qquad \text{(II. 2)}$$

Nilsson's nucleon wave functions are given in the isotropic harmonic oscillator representation with basis functions

$$\varphi_{nl}^{\Lambda}(\vec{r}) = (-1)^n \left[\frac{2\,n!\,\alpha^{3/2}}{(n+l+1/2)!}\right]^{1/2} (\alpha r^2)^{l/2} e^{-\frac{\alpha r^2}{2}} L_n^{l+1/2}(\alpha r^2)\, Y_l^{\Lambda}(\vartheta, \varphi), \qquad \text{(II. 3)}$$

where n is the number of radial nodes and equal to $(N-l)/2$, and $\alpha = \dfrac{m\omega_0}{\hbar}$ with m the nucleon mass and $\hbar\omega_0 = 41\,A^{-1/3}$ MeV chosen by NILSSON to give the proper nuclear size. $L_n^{l+1/2}$ is an associated Laguerre polynomial satisfying the equation

$$L_n^{l+1/2}(x) = \sum_k{}' (-1)^k \binom{n+l+1/2}{n-k} \frac{x^k}{k!},$$

where the $\binom{a}{b}$ quantity is a binomial coefficient in the usual notation. Ω is the projection of total angular momentum of the nucleon. Where a negative Ω value is involved, we will use the time-reversed wave function of positive Ω in order to have the correct phases for use with the pairing interaction formalism.

Approximate solutions of $(H-E)\,X = 0$ are

$$X_0 = \prod_{\Omega_p}{}' \prod_{\Omega_N}{}' (U_{\Omega_p} + V_{\Omega_p} a_{\Omega_p}^{+} a_{-\Omega_p}^{+}) \times (U_{\Omega_N} + V_{\Omega_N} a_{\Omega_N}^{+} a_{-\Omega_N}^{+}) \,|\, 0\rangle \qquad \text{(II. 4)}$$

in the case of an even-even nucleus, and the constants $U_{\Omega_p} V_{\Omega_p} U_{\Omega_N} V_{\Omega_N}$ are determined by the equations

$$U_{\Omega}^2 = \frac{1}{2}\left(1 + \frac{\varepsilon_{\Omega} - \lambda}{\sqrt{(\varepsilon_{\Omega} - \lambda)^2 + \Delta^2}}\right) \qquad \text{(II. 5a)}$$

$$V_{\Omega}^2 = 1 - U_{\Omega}^2 \qquad \text{(II. 5b)}$$

$$\frac{2}{G} = \frac{2}{\Delta} \sum_{\Omega>0}{}' U_{\Omega} V_{\Omega} = \sum_{\Omega>0}{}' \frac{1}{\sqrt{(\varepsilon_{\Omega} - \lambda)^2 + \Delta^2}} \qquad \text{(II. 5c)}$$

$$n = 2 \sum_{\Omega>0}{}' V_{\Omega}^2 = \sum_{\Omega>0}{}' \left[1 - \frac{\varepsilon_{\Omega} - \lambda}{\sqrt{(\varepsilon_{\Omega} - \lambda)^2 + \Delta^2}}\right], \qquad \text{(II. 5d)}$$

where n is the average number of particles (neutrons or protons) outside closed shells.

From (II. 4) we are able to calculate the functions G_{L0} for the decay of the ground state of an even-even nucleus to the ground-state band of the daughter nucleus.

$$G_{LO}(\mathrm{R}) = \prod_{\Omega_p} \prod_{\Omega_N} (U^i_{\Omega_p} U^f_{\Omega_p} + V^i_{\Omega_p} V^f_{\Omega_p}) \times (U^i_{\Omega_N} U^f_{\Omega_N} + V^i_{\Omega_N} V^f_{\Omega_N}) \sum_{\Omega_p \Omega_N}{}' \frac{V^i_{\Omega_p} U^f_{\Omega_p}}{U^i_{\Omega_p} U^f_{\Omega_p} + V^i_{\Omega_p} V^f_{\Omega_p}} \times \frac{V^i_{\Omega_N} U^f_{\Omega_N}}{U^i_{\Omega_N} U^f_{\Omega_N} + V^i_{\Omega_N} V^f_{\Omega_N}} \Gamma_{LO}^{\Omega_p - \Omega_p \, \Omega_N - \Omega_N}(\alpha, \beta, R) \qquad \text{(II. 6)}$$

$$\Gamma_{Lm}^{\Omega_1 \Omega_2 \Omega_3 \Omega_4} = R^{3/2} \int \mathfrak{A}(\varphi^{(1)}_{\Omega_1} \varphi^{(2)}_{\Omega_2}) \mathfrak{A}(\varphi^{(3)}_{\Omega_3} \varphi^{(4)}_{\Omega_4}) \times \chi_\alpha(\beta, \xi_\alpha) \, Y^m_L(\vartheta' \varphi') \, d\xi_\alpha \, d\Omega', \qquad \text{(II. 7)}$$

where $\mathfrak{A}$ means an antisymmetrization operator. The index i refers to the parent and f to the daughter nucleus.

Here we have written equation (II. 7) in a general manner that will apply also to unfavoured alpha decay. For favoured decay we are dealing only with paired nucleons, and the proton function $\varphi(2)$ is just the time-reversed wave function for $\varphi(1)$; similarly, for the neutron function $\varphi(3)$ and $\varphi(4)$. The first bracketed factor in (II. 6) together with the denominator of the next factor essentially brings in a decrease associated with the incomplete overlap between parent and daughter of the various pairs other than the pairs contributing to the sum. This "core overlap" factor will presumably not vary rapidly from nucleus to nucleus and will not affect relative intensities very much, unless one is at some discontinuity in orbital level spacing where there is a large change in the Fermi energy between parent and daughter. In deriving this factor it has been further assumed that the deformations of parent and daughter nucleus are the same. At any rate, in the numerical work to be reported in this paper, we have set all $U^i U^f + V^i V^f$ factors of (II. 6) to unity.

The numerators $V^i_{\Omega_p} U^f_{\Omega_p} V^i_{\Omega_N} U^f_{\Omega_N}$ provide the essential weighting factor for the contributions of the various orbital combinations to the sum $G_{LO}(R)$. This weighting factor is a measure of the probability that the given orbitals are occupied in the parent and vacant in the daughter. The factor attains a maximum value for orbitals with energies nearest the average of the parent and daughter chemical potentials, λ_i, λ_f, and the factor decreases for orbitals with greater or lesser energies.

Equations (II. 6) are quite general and define the $G_{LO}(R)$ functions throughout the nuclear volume. Thus, the $G_{LO}(R)$ functions along any desired connection surface S and their derivatives normal to that surface are calculable.

A Gaussian wave function is substituted for the alpha particle internal wave function and the integration over the internal coordinates is carried out as described in earlier work (Mang, 1960). The alpha size parameter β is related to the mean square radius of the alpha particle by the relation $\beta = \frac{9}{8} \frac{1}{\langle r^2 \rangle}$. The resulting formulas are the same as in an earlier report (Mang, 1959a) except that the angular momentum

factors are modified in the present use of the $|\,l\Lambda\Omega\,\rangle$ representation, whereas an $|\,lj\Omega\,\rangle$ scheme was previously used.

The integral of Eq. (II. 7), corresponding to a particular set of Nilsson orbital assignments for the protons (1, 2) and the neutrons (3, 4), has the following values:

$$\left.\begin{aligned} I_{Lm}^{\Omega_1\Omega_2\Omega_3\Omega_4}(\alpha,\beta,R) &= (-1)^f\left(\frac{2}{\alpha+\beta}\right)^{\frac{9}{2}}(\alpha\beta)^{\frac{9}{4}}\left(\frac{2\alpha}{\alpha+\beta}\right)^{\varrho_{\max}+\frac{L}{2}}\sqrt{2} \\ &\times\left(\frac{1}{2}!\right)^{-\frac{1}{2}}(\alpha R^2)^{\frac{3}{4}}e^{-2\alpha R^2}[2(\alpha+\beta)R^2]^{\frac{L}{2}}\sum_{\varrho}\left(\frac{\beta-\alpha}{2\alpha}\right)^{\varrho_{\max}-\varrho}C_{\varrho}^{L} \\ &\times L_{\varrho}^{L+\frac{1}{2}}(2(\alpha+\beta)R^2), \end{aligned}\right\} \qquad \text{(II. 8)}$$

where the Ω_i are the angular momentum projections and imply all additional indices needed to specify the particular Nilsson orbital. $\varrho_{\max}=\dfrac{(N_1+N_2+N_3+N_4-L)}{2}$, and the phase factor exponent f is the sum of $|\,\Omega_i\,|-1/2$ values for all orbitals with Ω_i negative.

The C_{ϱ}^{L} expansion coefficients do not depend upon α, β or R and are determined solely by the four nucleon wave functions as follows:

$$\left.\begin{aligned} C_{\varrho}^{L} &= \varrho!\,(2L+1)^{-\frac{1}{2}}2^{-(2\varrho+L)}\left(\frac{1}{2}!\right)^2\sum_{l_1l_2l_3l_4}[(2l_1+1)(2l_2+1) \\ &\times(2l_3+1)(2l_4+1)]^{\frac{1}{2}}\left[n_1!\,n_2!\,n_3!\,n_4!\left(n_1+l_1+\frac{1}{2}\right)!\left(n_2+l_2+\frac{1}{2}\right)!\left(n_3+l_3+\frac{1}{2}\right)!\right. \\ &\left.\times\left(n_4+l_4+\frac{1}{2}\right)!\right]^{-\frac{1}{2}}B_{\varrho}^{L}(n_i\,l_i)\sum_{\Sigma_1\Sigma_2\Sigma_3\Sigma_4}(-1)^{1-\Sigma_1-\Sigma_3+n_1+n_2+n_3+n_4} \\ &\delta_{\Sigma_1,-\Sigma_2}\,\delta_{\Sigma_3,-\Sigma_4}\,\alpha_{l_1|\Lambda_1|}\,\alpha_{l_2|\Lambda_2|}\,\alpha_{l_3|\Lambda_3|}\,\alpha_{l_4|\Lambda_4|}\,D(l_1\,l_2\,l_3\,l_4\,\Lambda_1\,\Lambda_2\,\Lambda_3\,\Lambda_4\,L) \end{aligned}\right\} \qquad \text{(II. 9)}$$

with

$$\Lambda_i+\Sigma_i=\Omega_i.$$

Our convention here is to take the Nilsson expansion coefficients $\alpha_{l\Lambda}$ for an orbital of negative Ω as identical (no sign change) to the corresponding coefficient in an orbital of positive Ω. There is no separate summation over the radial quantum numbers n, since the Nilsson wave functions do not have configuration admixture from other oscillator shells.

The D factor comes from the vector coupling conditions and is a sum over products of six Clebsch-Gordan coefficients.

$$\left.\begin{aligned} D(l_1 l_2 l_3 l_4 \Lambda_1 \Lambda_2 \Lambda_3 \Lambda_4 L) = \sum_{l_p l_N} & C(l_1 l_2 l_p;\ \Lambda_1 \Lambda_2) \\ & C(l_1 l_2 l_p;\ 00)\, C(l_3 l_4 l_N;\ \Lambda_3 \Lambda_4)\, C(l_3 l_4 l_N;\ 00) \\ & C(l_p l_N L;\ \Lambda_1 + \Lambda_2\ \Lambda_3 + \Lambda_4)\, C(l_p l_N L;\ 00). \end{aligned}\right\} \quad \text{(II. 10)}$$

It is interesting to note that the D function has just the value of the integral

$$\int Y_L^{*\Lambda_1 + \Lambda_2 + \Lambda_3 + \Lambda_4}\, Y_{l_1}^{\Lambda_1}\, Y_{l_2}^{\Lambda_2}\, Y_{l_3}^{\Lambda_3}\, Y_{l_4}^{\Lambda_4}\, d\Omega .$$

The B factor comes from the radial functions and is as follows:

$$\left.\begin{aligned} B_\varrho^L(n_i l_i) = (-1)^\varrho\, n_1!\, n_2!\, n_3!\, n_4! \sum_{\nu_1 \nu_2 \nu_3 \nu_4} & \frac{(-1)^{\nu_1 + \nu_2 + \nu_3 + \nu_4}}{\nu_1!\, \nu_2!\, \nu_3!\, \nu_4!} \\ \times \binom{n_1 + l_1 + \frac{1}{2}}{n_1 - \nu_1} & \binom{n_2 + l_2 + \frac{1}{2}}{n_2 - \nu_2} \binom{n_3 + l_4 + \frac{1}{2}}{n_3 - \nu_3} \binom{n_4 + l_4 + \frac{1}{2}}{n_4 - \nu_4}, \end{aligned}\right\} \quad \text{(II. 11)}$$

where the summation is restricted by

$$2\varrho + L = 2(\nu_1 + \nu_2 + \nu_3 + \nu_4) + l_1 + l_2 + l_3 + l_4 .$$

III. Numerical Computations: Input parameters and methods

In order to treat the alpha decay of Cm^{242} and its neighbours throughout the deformed region and yet keep the computing time on the IBM-709 computer reasonable we made a compromise choice of a set of 10 proton- and 10 neutron-orbitals centered about the Fermi energies appropriate to Cm^{242}. In Mottelson and Nilsson's (1959) proton level diagram (their Fig. 5) the orbitals chosen are the $1/2 + (660)$, $3/2 + (651)$ and successively higher orbitals at deformation $\eta = 5$ up through $7/2 - (514)$ and $9/2 + (624)$. For the neutrons (their Fig. 6) they are orbitals $3/2 - (761)$, $3/2 + (631)$, $5/2 - (752)$ and higher up to the gap at 152 neutrons.

In the first stage of computation the C_ϱ^L coefficients were evaluated according to Eq. (II. 9) and punched into cards. The only input data were the Nilsson coefficients which were taken, as a compromise, as the deformation $\eta = 4$ entries in the tables. It would have been desirable to have $\eta = 5$ wave functions, since this is a more typical deformation for the alpha emitters treated, but it was felt somewhat risky to attempt an interpolation of the Nilsson coefficients because of the probable need for more than two-point interpolation with greater chance for errors.

Computer programming was entirely in the FORTRAN II system except for use of a Clebsch-Gordan coefficient subroutine, kindly supplied by the Los Alamos Scientific Laboratory. Subroutines were written for Eqs. (II. 10) and (II. 11). In order to save computer time, factorials and binomial coefficients were stored in tables within

the memory. The coefficients were computed for L of 0,2, and 4 and for all 100 combinations of the 10×10 set of orbitals. The total computing time required for the approximately 3000 C_{ϱ}^{L} coefficients was about eight hours, not counting many times this amount of time spent testing, correcting, and retesting the programs.

The computer programs were thoroughly checked at many stages. One satisfying final check involved hand calculation of the $11/2-(505)$, $13/2+(606)$ combination. The program for C_{ϱ}^{L} coefficients was at first made to transform the Nilsson functions into an $|lj\Omega\rangle$ representation before calculations were performed using formulas based on Eq. (A 32) of MANG (1959a). This program was brought to completion and verified to give correct answers, but it was intolerably slow. Then, extensive reprogramming to treat the original Nilsson representation by Eq. (II. 9) of this paper was carried out. Ultimately, an order of magnitude improvement in program running speed was attained. The earlier slow program provided a valuable check against the new program, for a number of complicated orbital combinations were treated with both programs and found to give identical results at least to five significant figures.

To determine the quantities U and V of the pairing interaction, we have used mainly the Δ values determined by NILSSON and PRIOR (1961) from an analysis of odd-even mass differences. Orbital energy values were interpolated values for deformation $\eta = 5$ used by NILSSON and PRIOR in their moment of inertia calculations, and we are grateful to Dr. NILSSON for providing us with these unpublished tables of interpolated eigenvalues. The values of the chemical potentials, λ_p and λ_N, for various nuclei were calculated by an iterative computer program solving Eq. (II. 5d). The U and V values were then calculated from Eqs. (II. 5a) and (II. 5b). The orbitals and their energies assumed in this work are tabulated in Table I. The energies are given in units of $\varkappa\hbar\omega_0$ as in Nilsson's tables.

The evaluation of Eq. (II. 6) for $G_{LO}(R)$ was also carried out by the Lawrence Radiation Laboratory IBM-709 computer. In the calculation of G_{LO} for a particular nucleus the input quantities were as follows: (1) the 1000 C_{ϱ}^{L} coefficients on 300 cards, (2) the α value, (3) the β value, (4) the twenty orbital energies, and (5) four λ values and four Δ values for neutrons and protons in the parent and daughter nucleus. The program computed and printed out the 100 Γ_{LO} values from Eq. (II. 7), and also calculated the U and V values and the grand summation of (II. 6). The computing time for each G_{LO} was about two minutes.

We believe the best value for β to be $0.47 \times 10^{26}\,\mathrm{cm}^{-2}$, corresponding to the mean square radius of the He^4 nucleus of 1.55×10^{-13} cm, as measured by electron scattering (cf. HERMAN and HOFSTADTER, 1960). By mistake, a value of $\beta = 0.625$ was used for most of the computations. Several nuclei were recalculated with the value 0.47 with only small changes in the results, as can be seen in Tables V and VI.

The α value, which determines the nuclear size, is given by the equation

$$\alpha = \frac{m\omega_0}{\hbar}$$

TABLE I. Orbitals and their Energies Used for Calculations.

	Energy (units of $\varkappa\hbar\omega_0$)
Protons	
11/2 − (505)	− 20.000
1/2 + (660)	− 21.170
3/2 + (651)	− 19.833
1/2 − (530)	− 18.815
5/2 + (642)	− 17.705
5/2 − (523)	− 17.006
3/2 − (521)	− 14.753
7/2 + (633)	− 14.406
7/2 − (514)	− 12.328
9/2 + (624)	− 10.679
Neutrons	
13/2 + (606)	− 16.400
3/2 − (761)	− 20.013
3/2 + (631)	− 18.090
5/2 − (752)	− 17.958
5/2 + (633)	− 16.300
7/2 − (743)	− 15.176
1/2 + (631)	− 14.611
5/2 + (622)	− 13.278
7/2 + (624)	− 12.540
9/2 − (734)	− 11.789

with m the nucleon mass and $\hbar\omega_0$ the quantum energy in the harmonic nuclear potential well. We have chosen $\hbar\omega_0$ using NILSSON's (1955) relation $\hbar\omega_0 = 41\,A^{-1/3}$ Mev. For $A = 238$, the $\varkappa$ value is $0.1597\times10^{26}\,\mathrm{cm}^{-2}$. For simplicity, we have used this $\varkappa$ value for all the nuclei. The relevant parameter is $\varkappa R^2$ for the nuclear surface which should stay nearly constant for the various nuclei. A few calculations were run for a too small nuclear size ($\varkappa = .175$) in order to give insight into the sensitivity of the results on $\varkappa$.

Calculations were run at several R values for Th^{228} and Cm^{242}, and all other nuclei were calculated only at $R = 8.25\times10^{-13}$ cm (corresponding to the apparent inflection point in the $R^{-\frac{1}{2}}G_{LO}$ *vs.* R curves).

IV. Numerical Values of the G_{LO} Functions

Some interesting insight into the theoretical alpha probability functions G_{LO} are to be gained by examining the intermediate results $\Gamma_{LO}(\varkappa\beta R)$ for the contributions of the 100 different orbital combinations. Table II lists the relative values of Γ_{LO} for $L = 0$, $\varkappa = 0.1597$, $\beta = 0.47$, and $R = 8.25$. The entries of successive columns refer

TABLE II. Γ_{00} Relative Values.

L = O R = 8.25 $\beta = 0.47$ $\alpha = 0.1597$

Prot. $\Omega\,\Pi$ \ Neut. $\Omega\,\Pi$	$\frac{13}{2}+$	$\frac{3}{2}-$	$\frac{3}{2}+$	$\frac{5}{2}-$	$\frac{5}{2}+$	$\frac{7}{2}-$	$\frac{1}{2}+$	$\frac{5}{2}+$	$\frac{7}{2}+$	$\frac{9}{2}-$
$\frac{9}{2}+$	6	5	22	7	17	10	24	36	20	15
$\frac{7}{2}-$	7	4	13	5	10	7	14	24	13	9
$\frac{7}{2}+$	4	10	40	15	30	20	51	32	19	19
$\frac{3}{2}-$	9	27	77	34	58	39	103	72	42	37
$\frac{5}{2}-$	4	9	31	12	23	16	40	32	18	16
$\frac{5}{2}+$	3	23	43	29	33	24	72	22	13	14
$\frac{1}{2}-$	5	77	76	62	58	42	159	35	21	23
$\frac{3}{2}+$	2	46	31	34	25	17	76	14	9	8
$\frac{1}{2}+$	2	49	22	23	17	12	70	12	7	7
$\frac{11}{2}-$	16	2	5	2	4	3	6	10	6	4

to neutron orbitals and the rows to proton orbitals. We note that all entries are positive, a consequence of the time-reversal definition of relative phases of paired orbitals to insure all U and V values positive. It is to be seen that the lowest contributions generally come from the combination of an orbital of low Ω value (wave function large in polar region) with an orbital of high Ω value (large in equatorial region). Intuitively, we associate these low intrinsic contributions with the poor overlap of these functions.

Table III lists the corresponding values of Γ_{20} at the above α, β and R values. Here we note that all combinations are positive, except those involving the high-Ω strongly equatorial proton orbital 11/2-(505) and the neutron orbital 13/2+(606). This observation, too, is intuitively understood; those orbitals predominantly overlapping at polar latitudes $\vartheta' < \cos^{-1}\sqrt{1/3}$, where the Legendre function $P_2(\cos\vartheta')$ is positive, make positive contributions. In fact, the slope of an orbital in the Nilsson diagram measures a similar property. Roughly we may expect down-sloping orbitals to contribute positively to Γ_{20}, and vice versa.

TABLE III. Γ_{20} Relative Values.

L = 2 R = 8.25 $\beta = 0.47$ $\alpha = 0.1597$

Prot. $\Omega\,\Pi$ \ Neut. $\Omega\,\Pi$	$\frac{13}{2}+$	$\frac{3}{2}-$	$\frac{3}{2}+$	$\frac{5}{2}-$	$\frac{5}{2}+$	$\frac{7}{2}-$	$\frac{1}{2}+$	$\frac{5}{2}+$	$\frac{7}{2}+$	$\frac{9}{2}-$
$\frac{9}{2}+$	−10	5	27	8	20	12	33	11	7	11
$\frac{7}{2}-$	−11	1	9	2	6	4	12	1	1	0
$\frac{7}{2}+$	−7	24	74	37	55	41	108	36	22	25
$\frac{3}{2}-$	−16	74	146	88	109	79	238	61	38	47
$\frac{5}{2}-$	−6	21	56	29	41	30	85	25	15	19
$\frac{5}{2}+$	−5	83	110	92	84	63	210	34	22	26
$\frac{1}{2}-$	−10	310	201	215	155	115	528	58	36	43
$\frac{3}{2}+$	−4	188	93	124	74	52	274	20	13	15
$\frac{1}{2}+$	−3	218	62	88	49	33	277	15	10	11
$\frac{11}{2}-$	−37	−3	−8	−3	−6	−5	−9	−15	−8	−6

Table IV lists the relative Γ_{40} values taken from a calculation at the same α, β, and R values as for Tables II and III. We now note that combinations in the lower left-hand part of the table give positive contributions, and those in the upper right-hand part contribute negative Γ_{40} values. It is immediately apparent that $L = 4$ intensities will be determined in large measure by a cancellation of contributions that may vary rapidly with changing nucleon numbers. From Table IV we can note that a combination of extreme polar orbitals (any of the $\Omega_p = 1/2$, $\Omega_N = 1/2$ combinations) always gives a positive value, and a combination of extreme equatorial orbitals (e.g. 11/2 −, 13/2 +) gives a positive Γ_{40}. These results follow from the fact that the Legendre function is positive in the vicinity of $\vartheta' = 0$ and also $\vartheta' = \frac{\pi}{2}$.

Fig. 1 shows bar graphs of the weighting factors V_Ω (parent) U_Ω (daughter) for the contributions of the various neutron and proton orbitals. The orbital energies are to scale vertically, and the parent and daughter λ values are marked by dashed lines. It

TABLE IV. Γ_{40} Relative Values.

L = 4 R = 8.25 $\beta = 8.25$ $\alpha = 0.1597$

Prot. $\Omega\,\Pi$ \ Neut. $\Omega\,\Pi$	$\frac{13}{2}^+$	$\frac{3}{2}^-$	$\frac{3}{2}^+$	$\frac{5}{2}^-$	$\frac{5}{2}^+$	$\frac{7}{2}^-$	$\frac{1}{2}^+$	$\frac{5}{2}^+$	$\frac{7}{2}^+$	$\frac{9}{2}^-$
$\frac{9}{2}^+$	69	−241	−1235	−286	−937	−512	−1196	−2015	−1145	−884
$\frac{7}{2}^-$	15	−135	−607	−169	−470	−280	−588	−1295	−709	−486
$\frac{7}{2}^+$	64	−158	−1768	−286	−1312	−803	−1756	−1859	−1082	−1009
$\frac{3}{2}^-$	195	184	−3223	−342	−2384	−1427	−2731	−3969	−2260	−2028
$\frac{5}{2}^-$	71	−110	−1465	−242	−1080	−649	−1408	−1832	−1024	−929
$\frac{5}{2}^+$	47	788	−924	25	−670	−469	−261	−900	−533	−533
$\frac{1}{2}^-$	105	5212	−962	1631	−632	−506	3835	−1437	−825	−839
$\frac{3}{2}^+$	36	3278	124	1300	144	72	2931	−535	−296	−253
$\frac{1}{2}^+$	31	4822	−33	1192	33	−34	4743	−506	−284	−268
$\frac{11}{2}^-$	665	20	55	25	43	32	70	37	18	34

is apparent that the results for the lighter nuclei, such as Th^{228}, need improvement by inclusion of lower-lying orbitals, and we have eliminated Th from our final analyses. These calculations used mostly the orbitals that have been identified in the energy level systems of odd-A nuclei and hence appear on the simplified diagrams of the MOTTELSON-NILSSON work (1959). These diagrams fail to show many of the levels from adjacent major shells. The neglect of these primarily equatorial orbitals may well produce a systematic error of too great theoretical $L = 2$ intensities.

The function $R^{-1/2} G_{LO}$ as defined by Eq. (II. 5) may be considered the partial wave amplitude in the nuclear interior of the alpha particle of maximum kinetic energy (daughter nucleus ground state pairing function assumed) which must go over smoothly into the penetrating alpha wave of the decay process. In the simplest view of the Nilsson functions in the isotropic harmonic oscillator representation, the functions would define the α-wave function on a spherical surface as $\sum_L R^{-1/2} G_{LO} Y_L^0$. In our alpha decay calculations it is very important that we consider the Nilsson

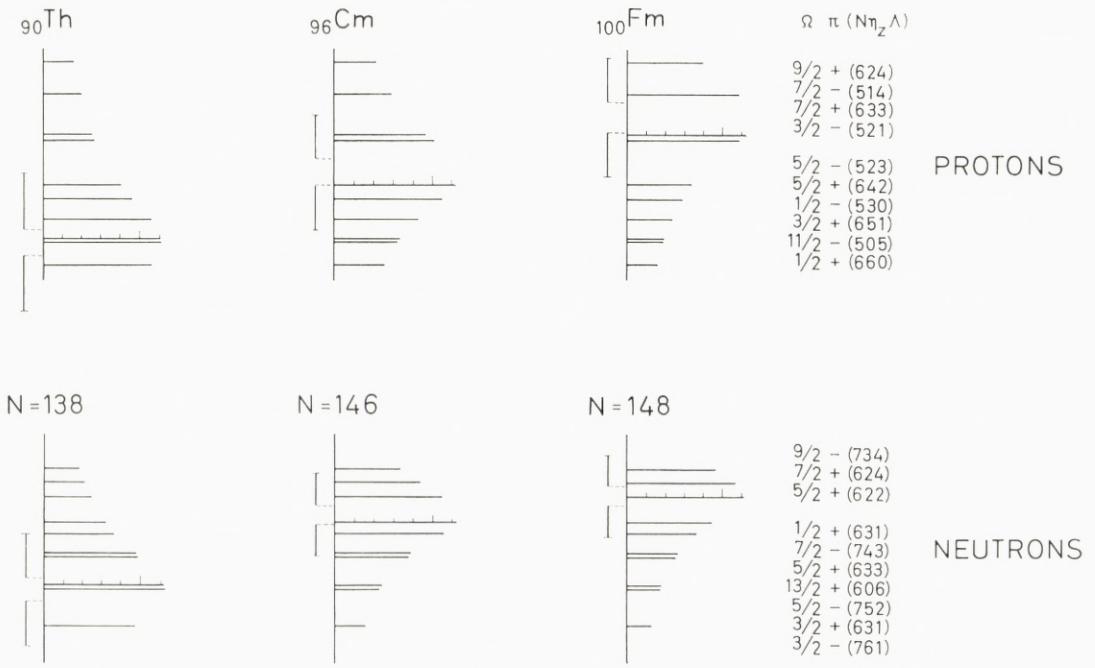

Fig. 1. Diagrams for three sample proton numbers and three sample neutron numbers where the energy of the Nilsson orbital is plotted to scale vertically and the lengths of the horizontal bars give the $u_i' v_i$ weighting factor for each orbital. (This factor is the square root of the probability that the orbital is occupied in the parent and vacant in the daughter.) The horizontal scale is indicated on the longest bar by marks every 0.1 unit. The vertical energy scale can be deduced from the vertical base lines which go from ε values of -22 to -10. The orbital energy for a proton orbital is then $(5+3/2+0.05\,\varepsilon_i)\,\hbar\omega_0$ and for a neutron $(6+3/2+.05\,\varepsilon_i)\,\hbar\omega_0$ with $\hbar\omega_0 = 41\,A^{-1/3}$ Mev. The orbital energies correspond to a deformation $\delta \sim 0.24$. To the left of the base line are dashed lines showing the positions of the chemical potential (or Fermi energy) for parent and daughter used in the calculation. The vertical bars extending from the ends of these reference lines are of length equal to the gap parameter Δ used for parent (upper) and daughter (lower). The size of Δ essentially establishes the energy width of the envelope of the $u_i' v_i$ values, with the envelope tending toward an asymptotic limit of

$$\frac{\Delta}{\sqrt{2}\,|\,\varepsilon_i - \lambda\,|}\,.$$

The orbitals used are listed with the usual asymptotic indices.

functions in the alternative representation described in his appendix *A* (Nilsson, 1955). This representation is superior in that Nilsson's neglect of wave function components from other major shells is much better justified. In the alternative representation, the radial coordinate surfaces are spheroids of half the deformation of the isopotential nuclear surface. For a nucleus of deformation δ we have to lowest order (where the subscript a denotes coordinates of a point (x, y, z) in the alternate representation) the following relations:

$$x_a = x\,(1 + \delta/6)$$
$$y_a = y\,(1 + \delta/6)$$
$$z_a = z\,(1 - \delta/3).$$

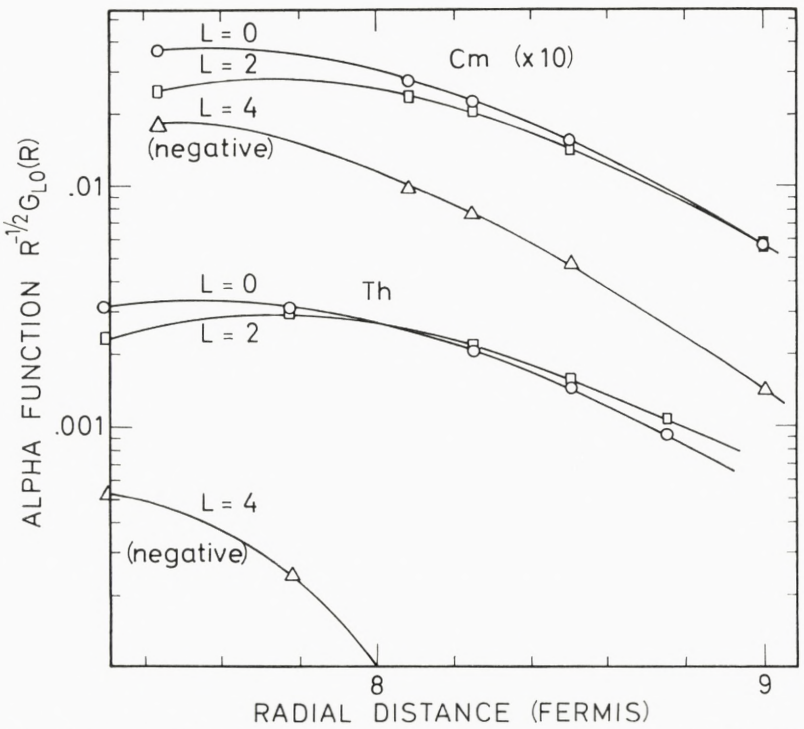

Fig. 2. Semi-logarithmic plot of the radial behaviour of the computed "internal" alpha-particle wave function $R^{-1/2}G_{LO}(R)$ for Cm^{242} and Th^{228} ($L=0$, ○; $L=2$, □; $L=4$, △). For the calculation were used $\alpha=0.1597$ and $\beta=0.625$. The values slightly differ from the functions and ratios tabulated in the text, because the radial behaviour here plotted comes from early calculations, using guessed values for the Fermi energies λ. The values in the text are later calculations using λ values as plotted in Fig. 1, which are solutions of the Belyaev equation $N=2\sum_i v_i^2$. The radial behaviour would be little affected by the slightly wrong λ values although the magnitudes of the functions are somewhat affected.
For Th^{228} the $L=4$ function is not graphed at large distance because it becomes too small to show and even changes sign.
A linear plot shows that the inflection points (zero curvature) are around $R=8.25$ f.

The first calculations to be made investigated the radial dependence of $G_{LO}(R)$ for Th^{228} and Cm^{242}. The G_{LO} functions were calculated at several different radii and at two different values of the nuclear size parameter α. Fig. 2 shows the variation of the $R^{-\frac{1}{2}}G_{LO}$ functions with distance for $\alpha=0.1597$ and $\beta=0.625$. The calculations at $\alpha=0.175$, corresponding to a nuclear size 5 % too small, are not plotted, but the results are very nearly the same at the same values of αR^2. Thus, a change of α mainly affects the distance scale. We have in general performed our calculations over a range of nuclei using constant values of α and R with this justification.

The larger functions $R^{-1/2}G_{00}$ and $R^{-1/2}G_{20}$ at the outermost distances show a radial behaviour similar to that of the most lightly bound nucleon wave functions. The outer inflection points $\sim 8.2\times10^{-13}$ cm occur at about the distance of the classical turning points of these nucleon orbitals in the harmonic potential. The fall-off outside the

Table V. G_{LO} Value Ratios.

Alpha ..... Emitter.....		G_{20}/G_{00} G_{40}/G_{00}	
	α = .1597 β = .47 R = 8.25	α = .1597 β = .625 R = 8.25	α = .1597 β = .625 R = 8.5
Th^{228}	1.110	1.092	1.133
	.049	.058	.095
U^{230}	..	1.075	..
	..	+.004	..
U^{232}	..	1.040	..
	..	−.047	..
U^{234}	..	1.013	..
	..	−.085	..
U^{236}	..	1.004	..
	..	−.113	..
Pu^{238}	..	.976	..
	..	−.187	..
Pu^{240}	..	.945	..
	..	−.240	..
Cm^{242}	.919	.887	.926
	−.340	−.352	−.318
Cm^{244}	.848	.818	..
	−.428	−.438	..
Cf^{246}	.786	.758	..
	−.525	−.531	..
Fm^{248}	.736	.708	..
	−.575	−.580	..

inflection points is more rapid than exponential, like the behaviour of the nucleon functions in the rapidly rising harmonic potential. In fact, this overly-rapid, Gaussian-like fall-off is an unrealistic property of the harmonic oscillator wave functions. Radial wave functions in a more realistic square well-like potential show more nearly a simple exponential fall-off at outer distances. Harada (1961) has investigated this question and the effects on alpha decay rate calculations of spherical nuclei.

For two reasons we prefer to modify and approximate the calculated outermost radial dependence of $R^{-1/2}G_{LO}$ functions by a simple exponential dependence as it would be with a square well potential. First of all, this modification offers a means of approximately remedying the too-repulsive harmonic potential at large distances, and secondly, the exponential dependence simplifies the transformation of the G_{LO} vector from the spheroidal surface of constant radial parameter R_0 over to the more eccentric spheroidal surface of constant nuclear density at which the external solution is to be joined.

We have made a comparison between rounded square well wave functions

Table VI. Absolute G_{00} Values.

Alpha emitter	$G_{00}\times 10^2$		
	$\alpha = .1597$ $\beta = .47$ $R = 8.25$	$\alpha = .1597$ $\beta = .625$ $R = 8.25$	$\alpha = .1597$ $\beta = .625$ $R = 8.5$
Pu^{238}	..	.67	..
Pu^{240}	..	.64	..
Cm^{242}	.67	.628	.439

(Blomqvist and Wahlborn, 1960) and the harmonic oscillator wave functions and have concluded that a reasonable way to improve the H.O. wave functions would be to smoothly join a simple exponential to the H.O. wave function at its inflection point. Thus, we shall adopt the procedure of replacing the $R^{-1/2}G_{LO}$ functions by a simple exponential, tangent to the H.O. wave function at its inflection point (near $R = 8.2$).

Of course, the behaviour of the small G_{40} in Th^{228} which changes sign at $R = 8.2$ is not well approximated by an exponential, but its small magnitude, relative to G_{00} and G_{20}, makes the errors produced by the exponential approximation in the final answers quite unimportant.

Table V lists the G_{LO} values relative to G_{00}; it is only the ratios that enter into the calculations of final relative intensity of alpha groups to various rotational states. Fortunately, it appears that the results are not too sensitive to the exact choice of parameters. Thus, we shall use the most complete set of calculations, that of the middle column, for our further calculations, although the β value of 0.47 of the first column of results actually corresponds best to the size of the alpha particle in free space. The ratios are seen to have a smooth behaviour from one nucleus to the next heavier nucleus.

Table VI lists the absolute G_{00} values for a few nuclei whose Fermi energies lie toward the middle of the energy range of the nucleon orbitals used in the calculation. The absolute values and their trends can only be expected to have meaning for such nuclei.

V. Theoretical Intensity Values

Before we can calculate theoretical alpha decay intensities we must transform the G_{LO} expansion into a Legendre expansion on the spheroidal connection surface. That is, we must evaluate the integral of Eq. (I. 16). For this it is most convenient to have a simple approximate functional form for the radial dependence of the functions just beyond their inflection points.

We shall assume that the radial dependence in the vicinity of $R = 8.375f$ is just a simple exponential joining the calculated functions smoothly at this distance. Such

behaviour means a slower fall-off than calculated at large distance, but is really more appropriate for a finite-well nuclear potential

$$R^{-1/2} G_{LO}(R) = R_0^{-1/2} G_{LO}(R_0) \exp\left[-\gamma_L \cdot \frac{R - R_0}{R_0}\right]. \tag{V. 1}$$

To join smoothly we take γ_L as a dimensionless logarithmic derivative of $R^{-1/2} G_{LO}$ at $R = 8.375$. From the calculated G_{LO} values for Cm^{242} at $R = 8.25$ and $R = 8.5$ we get by finite difference $\gamma_0 = +12.6$, $\gamma_2 = +11.3$, and $\gamma_4 = +16.4$. We shall use these γ_L values also for other nuclei, though we only have investigated radial variations for one other, Th^{228}, with nearly the same result for γ_0 and γ_2 and somewhat different for the small G_{40}.

Let us consider that the nuclear surface on which connection is to be made is given by the equation

$$\left.\begin{aligned} R_s(\vartheta') &= R_c\left[1 + \frac{2\delta}{3} P_2(\cos\vartheta')\right] + R_0 - R_c \\ &= R_0\left[1 + \frac{2\delta_f}{3} P_2(\cos\vartheta')\right], \end{aligned}\right\} \tag{V. 2}$$

where

$$\delta_f = \frac{R_c}{R_0}\,\delta.$$

R_c is the equivalent radius $1.2 \times 10^{-13} A^{1/3}$ cm for which the δ values of Prior and Nilsson (1961) were calculated using experimental Q_0 values. R_0 is the radius $1.37 \times 10^{-13} A^{1/3}$ cm (i.e., $8.5f$ for Cm^{242}) slightly beyond the inflection point of the G_{LO} functions at $8.25f$, the radius at which most of our calculations were made. We feel that the above choice of the connection surface is a good estimate of the surface on which the effective alpha-particle potential is constant, aside from $P_4(\cos\vartheta')$ deformations discussed later. The assumption is essentially that the effects, such as diffuseness of the nuclear density distribution and finite range of nuclear forces, act to position the beginning of the alpha barrier at a constant distance $(R_0 - R_c)$ from the surface of the uniformly charged spheroid giving the proper experimental mean square radius and intrinsic quadrupole moment. It is troublesome that the real part of the Igo optical-model potential would make the barrier begin still about one Fermi further out than our R_0. We feel that this discrepancy is due to remaining defects in the Hamiltonians describing both inner and outer regions. In order to apply our formulations of Section I we need to alter the external potential from the Igo potential so that the alpha barrier begins at the inflection point of our G_{LO} functions. Fortunately, the theoretical *relative* intensities we calculate will be nearly independent of the detailed way in which the Igo potential is altered, but the absolute transition probabilities we calculate will be subject to uncertainty.

As pointed out in the first section, it is desirable to carry out the connection of

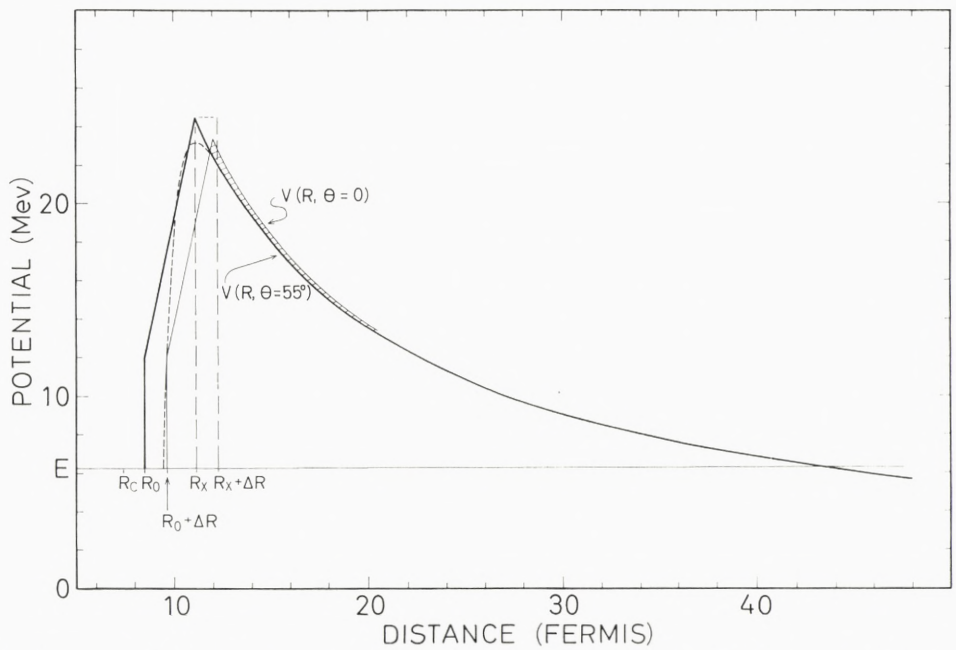

Fig. 3. Plots to scale of the potential profiles of the assumed barrier for Cm^{242} along $\theta = 55°$ (i.e. the zero of $P_2(\cos\theta)$) and along the polar axis $\theta = 0°$. The continuous curve gives the Igo real potential for comparison. Several radial distances are noted, R_c, the effective charge radius $1.2\times10^{-13}A^{1/3}$.
R_0, the chosen connection radius between internal and external solutions.
$R_0+\Delta R$, the distance of the connection surface at $\theta = 0$.
$\left(\Delta R = \frac{2}{3}\delta Rc\right)$.
R_x is the barrier peak along $\theta = 55°$, chosen to match the Igo barrier peak.
The horizontal line E marks the alpha distintegration energy.

inner and outer solutions within the barrier region, because one wishes the WKB approximation to be valid for the external solution and wishes to be able to neglect centrifugal barrier effects near the nucleus in treating the anisotropic barrier problem.

We shall make use of the Fröman matrix method (1957) in dealing with the barrier transmission, but we shall carefully reexamine the problem to determine the arguments of the matrices, using a diffuse nuclear potential and basing the relationship between experimentally determined Q_0 values and inferred deformation parameters on nuclear charge distributions of the correct size. In order to have a definite diffuse anistropic potential for analysis we assume, based on the curvature of the G_{LO} functions at R_0, that the potential energy is 12 Mev on the surface $R_s(\vartheta')$ defined by (V. 2) and that the barrier maximum comes at the average distance $11.1f$, which is the barrier top obtained using the Igo potential. (Fortunately the barrier treatment here is quite independent of the constant potential assumed at R_s.) We let the potential experienced by the alpha particle rise linearly with distance from $R_s(\vartheta')$ for all angles ϑ' until it intersects the pure Coulomb potential

$$V_c - \frac{2\,Ze^2}{R} + \frac{Q_0\,e^2}{R^3}\,P_2(\cos\vartheta').$$

From the intersection surface outward the potential is taken as purely coulombic.

Fig. 3 plots the potential profiles along $\vartheta' = 55°$ (where $P_2(\cos\vartheta')$ vanishes) and along $\vartheta' = 0$. The Fröman matrix method divides the wave propagation through the barrier into two stages, first, the propagation from the spheroidal surface $R_s(\vartheta')$ to a spherical surface and, second, the propagation from the sphere outward to infinity. We shall choose the spherical surface to be just beyond the range of the nuclear force, i.e., $R_x + \Delta R$ in Fig. 3. The appropriate argument B for the Fröman matrix is just the value of the WKB barrier integral along $\vartheta' = 55°$ minus the value of the integral along 0°.

Before considering the Fröman matrix further let us consider the transformation from the coordinate system of the nucleon to the isopotential connection surface.

The surface integral of Eq. (I. 16) accomplishes this transformation and may now be evaluated using (V. 1) and (V. 2)

$$\int Y_{l'}^{0\,*}\frac{G_{LO}}{R_s^{1/2}}\,Y_L^0\,d\Omega' = \int Y_{l'}^{0\,*}\exp\left[-\frac{2}{3}\,\delta_f\gamma_L P_2(\cos\vartheta')\right]Y_L^0\,d\Omega' \times R_0^{-1/2}\,G_{LO}(R_0). \qquad \text{(V. 3)}$$

The exponent above would be obtained if the G_{LO} were expansion coefficients in spherical polar coordinates. As we have pointed out in the preceding section, it is important to consider that the expansion is in Nilsson's alternate representation of modified scale parameter. Taking this into account and noting that the integrals are now just identical to the definition of a Fröman matrix element, we have

$$\int Y_{l'}^{0\,*}\frac{G_{LO}(R_s)}{R_s^{1/2}}\,Y_L^0\,d\Omega' = k_{l'L}(B_L)\,R_0^{-1/2}\,G_{LO}(R_0) \qquad \text{(V. 4)}$$

with

$$B_L = -\frac{\gamma_L}{3}(2\,\delta_f - \delta) = -0.27\,\delta\gamma_L.$$

If we take a weighted average γ value of about 12, we have the approximate expression

$$B_L \approx -3.2\,\delta.$$

At the end of Section I it was pointed out that the matrix element $B_{lj}^{l'm'}$ simplified in the even-even case to a Fröman matrix element times a reciprocal irregular Coulomb function. Since the product of two Fröman matrices is the matrix whose argument is the sum of those of the factors, we shall be able to write Eq. (I. 16) in a simple form:

$$\lambda_l = \frac{v_l}{R_0\,G_l^2(\eta_l, \varrho_{lo})}\left|\sum_L k_{lL}(B_q + B_s + B_L)\,G_{LO}(R_0)\right|^2. \qquad \text{(V. 5)}$$

B_s is the argument of the matrix that transforms the expansion on the connection surface (V. 2) to the spherical surface at $R_x + \Delta R$ just beyond the range of nuclear forces. B_q is the argument of the matrix transforming the expansion on the sphere to the expansion near the classical turning point. In analogous fashion to FRÖMAN we get the following expression:

$$B_s \approx \frac{2}{3} \delta k_0 R_c \left(\frac{2\eta}{k_0 R_x} - 1 \right)^{1/2}, \tag{V. 6}$$

where R_x is the radial distance at the barrier maximum

$$B_q \approx -\frac{q}{6\eta^2} \left(\frac{2\eta}{k_0 (R_x + \Delta R)} - 1 \right)^{1/2} \left(1 + \frac{\eta}{k_0 (R_x + \Delta R)} \right), \tag{V. 7}$$

where the symbols have been defined in connection with Eq. (I. 19). The parameter q, the dimensionless quadrupole coupling constant, can be rewritten

$$q = \eta \frac{k_0^2 Q_0}{Z} = \frac{2 M k_0 Q_0 e^2}{\hbar^2}.$$

Thus, we may rewrite B_q

$$B_q = -\frac{k_0^2 Q_0}{6 Z} \left(\frac{2\eta}{k_0 (R_x + \Delta R)} - 1 \right)^{1/2} \left(\frac{1}{\eta} + \frac{1}{k_0 (R_x + \Delta R)} \right).$$

In Fig. 3 the nature of the approximation can be seen. B_s is the WKB integral over the rectangular region of width ΔR and height the coulombic potential at R_x. B_q is the integral over the barrier difference shown by the small shaded region. To get a simpler approximate expression for B arguments we may substitute parameters for our average alpha emitter Cm^{242}.

$$\eta = 23.7$$

$$k_0 = 1.085 f^{-1}$$

$$R_c = 7.45 f$$

$R_x = 11.1 f$, using the real part of IGO's potential.

Then,

$$B_s \approx 9.30 \delta$$

$$B_q \approx -0.045 Q_0.$$

The total argument is

$$B = B_q + B_s + B_L \approx 6.1 \delta - 0.045 Q_0. \tag{V. 8}$$

We have used Eqs. (V. 5) and (V. 8) to calculate relative intensities from the G_{LO} relations of the central column of Table V.

Table VII. Experimental and Theoretical Reduced Wave Amplitudes assuming only Quadrupole Surface Deformation.

Alpha emitter	δ daughter	Q_0 daughter (10^{-24}cm^2)	B	Theory				Experiment	
				b_2	b_4	b_{4i}	b_4	b_2	b_4
U^{230}	.195	8.20	0.82	1.26	0.34	−.130	.37	1.36	.70
U^{232}	.199	8.47	0.83	1.23	0.29	−.112	.31	1.31	.60
U^{234}	.205	8.74	0.86	1.22	0.27	−.106	.29	1.23	.63
U^{236}	.214	9.26	0.89	1.21	0.25	−.107	.27	1.22	.62
Pu^{238} ...	.219	9.80	0.90	1.18	0.18	−.105	.21	1.08	.22
Pu^{240} ...	.229	10.35	0.93	1.16	0.14	−.121	.19	1.02	.26
Cm^{242}...	.236	10.96	0.95	1.10	+0.022	−.112	.114	0.99	.12
Cm^{244}...	.240	11.20	0.96	1.02	−0.08	−.100	.13	0.93	.08
Cf^{246}....	.243	11.70	0.95	0.97	−0.20	−.105	.226	0.84	.19
Fm^{248}...	.243	12.00	0.94	0.91	−0.28	−.103	.30	..	..
Fm^{254}...	..	..	..	..	..	..	..	.70	0.30

Table VII lists the final calculations of reduced relative intensities b_2 and b_4 compared with experiment. These quantities are defined exactly in accordance with Fröman

$$b_l = \frac{\sum_L k_{lL} G_{LO}(R_0)}{\sum_L k_{OL} G_{LO}(R_0)}. \qquad \text{(V. 9)}$$

They are the square roots of reciprocals of the reduced hindrance factors. The δ values are taken from Nilsson and Prior (1961) and the Q_0 values calculated by their quadratic relationship with these values, using the nuclear radius $1.2A^{1/3}f$.

There is a further correction which is not negligible for very weak groups. That is essentially the Coulomb excitation process occurring primarily beyond the classical turning point. The effect may be approximated by a small imaginary component in the argument of the Fröman matrix as Nosov (1957) has done. The calculation of this correction is discussed in the Appendix. The b_{4i} of Table VII is given as follows:

$b_{4i} = b_2 \hat{k}_{24} \times$ (penetrability factor of $L = 2$ divided by the penetrability of $L = 4)^{1/2}$ with $\hat{k}_{24}$ given by the equation of the Appendix, including the correction for finite nuclear rotational energy.

The proper $|b_4|$ reduced amplitude to compare with the experimental is

$$|b_4| = \sqrt{b_4^2 + b_{4i}^2}.$$

The Coulomb excitation components of the abundant $L = 0$ and $L = 2$ groups are quite negligible and have not been calculated.

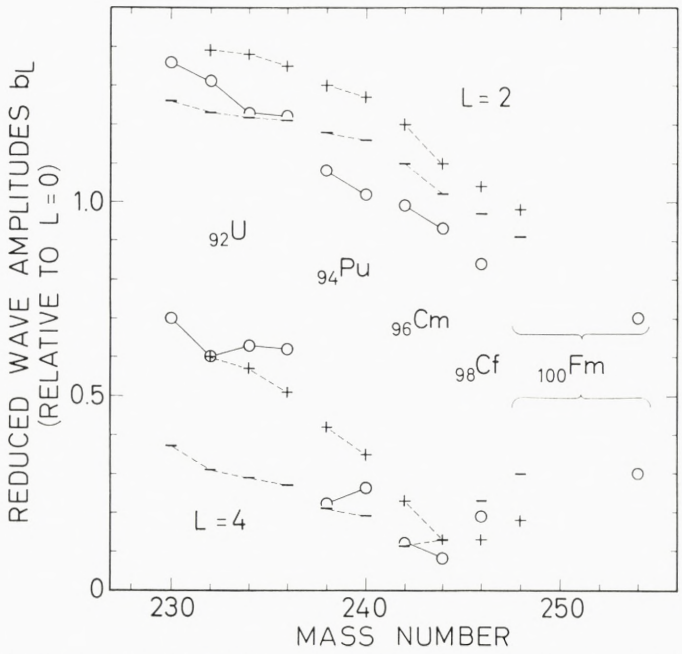

Fig. 4. Comparison of experimental (○) and theoretical reduced wave amplitudes $|b_L|$. The values for a given element are connected by lines, solid for experiment, dashed for theoretical. The theoretical values marked by bars (−) are for no $P_4(\cos\vartheta')$ deformation and those with crosses (+) are corrected for such deformation.

There is also a second set of theoretical points plotted in Fig. 4. These points correspond to values approximately corrected for 2^4-pole deformation of the nuclear surface. KJÄLLQVIST (1958) has calculated theoretically the magnitude of the surface deformation term $\beta_4 Y_{40}(\Theta')$. To treat the higher order deformation properly would involve a Fröman-type matrix with elements of the form

$$\int Y_l^{0*} \exp\left[BP_2(\cos\vartheta') + DP_4(\cos\vartheta')\right] Y_L^0 \, d\Omega',$$

and this matrix would not exactly factor into a product of matrices depending separately on quadrupole and 2^4-pole deformation. To first order in β_4, and following similar considerations to FRÖMAN (1957) and those used earlier here in deriving approximate expressions for B_L and B_s, we make a correction for P_4 deformation by multiplying the G_{LO} (real) vector by a square matrix whose elements are

$$f_{lL} = \delta_{lL} + \frac{9.15\,\beta_4}{\sqrt{4\pi}} C^2(l\,4\,L;\,00) \sqrt{\frac{9\cdot(2l+1)}{2l+1}}.$$

The corresponding corrected wave amplitudes are given in Table VIII.

Table VIII. Theoretical Reduced Wave Amplitudes Corrected for $P_4(\cos\vartheta')$ Deformation of the Nuclear Surface.

Alpha emitter	(theo.) β_4	b_2	b_4	b_{4i}	$\lvert b_4 \rvert$
U^{230}	No β_4 value available for daughter				
U^{232}	.062	1.39	.59	−.12	.60
U^{234}	.061	1.38	.56	−.12	.57
U^{236}	.053	1.35	.50	−.12	.51
Pu^{238}	.048	1.30	.40	−.12	.42
Pu^{240}	.043	1.27	.33	−.13	.35
Cm^{242}	.042	1.20	.20	−.12	.23
Cm^{244}	.038	1.10	.07	−.11	.13
Cf^{246}	.035	1.04	−.07	−.11	.13
Fm^{248}	.036	0.98	−.15	−.11	.18

The Kjällqvist β_4 values are all positive and range monotonically downward from 0.062 at Th^{228} to 0.022 at Cf^{250}. The correction matrix element of most importance to us is the f_{04}, which acts to add a positive contribution to the $l = 4$ amplitude.

Since there are no direct experimental measurements of 2^4-pole deformation, it is satisfying to see that the effects of such a deformation on our calculations are not so drastic as to invalidate it. Nevertheless, the effects of 2^4-pole deformation of the isopotential surface clearly cannot be neglected for really quantitative future theoretical calculations.

Fig. 4 plots the magnitudes of the relative reduced amplitudes. The theoretical results reproduce the essential features of the experimental values with the minimum in $|b_4|$ and with the gradual fall-off of $|b_2|$.

If the results of Fig. 4 are compared with the figure of the preliminary paper on this work (Mang and Rasmussen, 1961), some differences are noted. The preliminary results did not take into account the Coulomb excitation component of $l = 4$, which is significant for the cases of nearly vanishing b_4. More important, the preliminary results were calculated using larger arguments for the Fröman matrix based on the formula $B \approx 6.0\,\delta$ rather than Eq. (V. 8) of $B = 6.1\,\delta - 0.045\,Q_0$. The larger B values threw the minimum in b_4 into element 98, at a higher atomic number than experimental. The results of Fig. 4 show the theoretical minimum to be now somewhat on the other side of experimental. The theoretical $|b_2|$ values of Fig. 4 show generally some reduction as a consequence of the lowered B value.

In part the smaller B value expression of Eq. (V. 8) results from the consideration of a sloping nuclear potential, but the difference comes mainly from our inexact procedure in the preliminary work of using the deformation values of Nilsson and

Prior (1961), based on a charge radius of $1.2 \times 10^{-13} A^{1/3}$ cm with Fröman's Eq. (VIII-6), which was derived on the basis of a charge radius of $1.44 \times 10^{-13} A^{1/3}$ cm. The relative intensities of $l = 4$ are seen to be rather sensitive to the anisotropic barrier penetration effects dealt with by the Fröman matrix. Of course, there are still uncertainties with our present formula (V. 8), but it is probably more nearly correct than the expression used in the preliminary paper.

The agreement of theory with experiment in Fig. 4 is clearly so encouraging that we feel it established that the wave function of alpha particles contributing to alpha decay undergoes angular variation over the deformed surface in essentially the same way as the nucleon orbitals near the Fermi surface.

We may confidently use the results of our calculations to decide in most cases which is the correct one of the several possible results of inward integrations based on experimental intensities, deciding the phase ambiguity through $L = 0$, 2, and 4. For example, in Pennington and Preston (1958), four possible phase cases are depicted from inward numerical integrations of several nuclei from U^{234} through Fm^{254}. Our work would now categorically rule out cases III and IV, with their large negative $L = 2$ amplitudes. Further, we would select case I for the nuclei below Cm^{242} and case II for those heavier than Cm^{242}, with the choice between cases I and II being uncertain for Cm^{242} itself. Our theoretical prediction of positive $L = 2$ phase is indirectly confirmed by several angular correlation experiments involving favoured decay of odd-mass nuclei, but no experiments have yet measured our prediction that $L = 4$ is in phase below curium and out-of-phase for heavier elements.

That the $L = 4$ minima of theory and experiment coincide at element Cm is somewhat fortuitous; the inclusion of more $\Omega = 1/2$ orbitals at lower energy might displace the minimum toward higher Z. Also the inclusion of G_{60} in future calculations will probably affect the location of the $L = 4$ minimum.

The inclusion of the above-mentioned $\Omega = 1/2$ orbitals would probably also increase somewhat the $| b_2 |$ values mostly for uranium. The inclusion of more of the orbitals from the next lower major shell (only one $h\,11/2$ proton orbital and one $i\,13/2$ neutron orbital were used here) would tend to lower the $L = 2$ amplitudes.

Perhaps the contribution to the alpha-decay amplitude from orbitals in neighbouring closed shells would tend to contribute rather uniformly over the nuclear surface and enhance $L = 0$ relative to $L = 2$.

In contradistinction to the interpretation of spheroidal nuclear alpha intensity patterns as arising from a non-uniform alpha amplitude over a constant-matter-density surface, there has been an alternative approach relating the patterns uniquely to the shape of the nuclear surface (Fröman, 1957; Gol'din, Novikova, and Ter-Martirosyan, 1959; Gol'din, Adel'son-Velskii, Birzgal, Pilia, and Ter-Martirosyan (1958); Nosov, 1957; Strutinsky, 1957). Such theories are based on the assumption that the alpha amplitude over the nuclear surface is constant. These treatments give the correct $L = 2$ phase and nearly the correct magnitude for the quadrupole deformations, since the dominant influence on the alpha penetration is the thin barrier in the

polar region. When calculating finer details, the assumption of a strictly constant alpha wave function over the surface (i.e., over the isopotential surface for alpha) may cause difficulties. These treatments generally lead to quadrupole deformation parameters that decrease with mass number through the region of deformed nuclei, in conflict with experimental and theoretical evidence as shown, for example, by SZYMAŃSKI (1961). Small amounts of P_4 deformation of the spheroidal surface are also needed to explain the intensity patterns observed, but the negative β_4 values required near Curium seem in complete conflict with the shell model β_4 estimates (KJÄLLQVIST, 1958).

We would suggest a modified version for an alpha decay model solely related to shape parameters—one which is more in line with the spirit of our shell model treatment and is more likely to give reasonable results. That is, the alpha wave function over the deformed isopotential surface should vary in accordance with the *change* in nuclear matter density between parent and daughter. That is, the Y_{20} component of the alpha wave on the surface should be proportional to the change in quadrupole deformation and the Y_{40} component to the change in β_4 between parent and daughter. It is beyond the scope of this paper to make here a quantitative test of such a new model, but it does seem physically reasonable and could relate alpha relative intensities and shape parameters so as to be consistent with SZYMAŃSKI's β_2 and KJÄLLQUIST's β_4 values.

Our theoretical computations may be used also to calculate absolute decay rates, although such calculations depend much more sensitively than the relative rates upon detailed assumptions about the attractive nuclear potential felt by the alpha within the inmost part of the barrier. We make a rough estimate for the ground state decay of Cm^{242} by assuming the penetrability 2.16×10^{-27} from calculations using the Igo potential (RASMUSSEN, 1958). From Table VI we have $G_{00} = 0.0063$ at its inflection point at $R = 8.25$. Using Eq. (III. 4) we calculate an absolute decay rate 65 times less than experimentally observed. This absolute rate calculation is really uncertain. If we were to be consistent with the barrier assumptions made for the analysis of the relative transition rates, we would be thickening the barrier by bringing it in closer by about one fermi compared with the Igo potential, and the discrepancy with experiment would be greater than the factor 65 quoted above.

Qualitatively, it seems clear that our shell model formulation of alpha decay is giving us absolute decay rates too low, but it is quite uncertain just how much we fall short. Because of the great sensitivity of rate to barrier thickness it may be difficult ever to test a model of alpha decay really quantitatively in absolute rates. It would be of great value in this respect to have more optical-model analyses of alpha elastic (and rotational inelastic) scattering, particularly at energies below 40 Mev. Then the alpha decay theorist might have a potential he could extrapolate with greater confidence into the energy region of alpha decay.

The pairing interaction was an important addition in bringing in neutron correlations and proton correlations separately, but influence of neutron-proton forces

in bringing about correlations enhancing the alpha cluster is as yet not included. The proton motion in our treatment is completely uncorrelated with neutron motion.

We have examined the effect of the pairing correlation on absolute decay rate by comparing the G_{00} for Cm^{242} with the average of the G_{00} values which would replace G_{00} values in the limit $\Delta \to 0$, no pairing interaction. The actual G_{00} is 18 times the average and even 2.9 times the Γ_0 corresponding to the most favourable combination of orbitals considered (i.e., $1/2-(530)$ protons, $1/2+(631)$ neutrons). The effect of pairing on the decay rate is the square of the above number, an enhancement of a factor of 320. Thus, we see clearly that the pairing correlation not only smooths out the great fluctuations in decay rate for various nuclei that would obtain in the absence of pairing, but it also greatly enhances the decay rate. We have made a rough estimate of the further enhancement to be obtained by using all orbitals of three oscillator shells, as NILSSON and PRIOR (1961) did, and find about an additional factor of 4. This rough estimate is based on a suggestion by MOTTELSON to use the relationship $\frac{\Delta}{G} = \sum_{\Omega} u_\Omega v_\Omega$. There is perhaps also to be expected some increase if the harmonic oscillator radial wave functions were to be replaced by more realistic functions in a WOODS-SAXON potential (1954); (BLOMQVIST and WAHLBORN, 1960). We have partially corrected our work in this regard by fitting exponentials to the G functions at their outermost inflection points.

Perhaps the external Hamiltonian is at fault, too. It is well known that the optical-model potentials for neutrons and protons are energy-dependent, with the real part becoming less attractive with increasing kinetic energy. If the same trend were to hold for alpha particles, the barrier might be thinner than is given by the optical potential for 40 Mev alphas. Also we have in the external Hamiltonian neglected all coupling between alpha particle and nuclear internal degrees of freedom aside from nuclear rotation. Inclusion of further couplings can also effectively enhance the barrier penetrability for the ground-band decay.

Despite the failure to match experimental decay rates absolutely, can anything be said from our results about trends of absolute transition probabilities from nucleus to nucleus? We must be cautious about drawing conclusions from the trends of the G_{00} values at constant αR^2 in Table VI, because of the limited span of orbital energies compared to Δ. Because of the great G_{00} enhancement due to pairing correlation we should expect to see a spurious fall-off of G_{00} as the Fermi energy approaches any of the outer limits of our range of orbital energies. The decrease with mass number seen in Table VI probably comes mainly from the use of Δ values decreasing with proton and with neutron number.

We cannot make quantitative calculations, but with some of our results as a guide we can discuss matters qualitatively. Thus, the Nilsson orbital density near the Fermi energy should directly affect the absolute alpha transition probabilities in that a high density results in a larger Δ and the participation of more orbitals in the collective enhancement of the alpha amplitude.

A second factor may be inferred from examination of Γ_{00} and Γ_{20} values in Tables II and III. The $\Omega = 1/2$ orbitals seem especially effective in contributing to alpha decay in exhibiting large Γ_{00} values. A third general factor has been discussed by several authors and involves the increased penetrability expected for increasing deformation.

The first-factor dependence would suggest that there might be a direct correlation between the odd-even mass difference (which measures Δ) and the reduced alpha transition probability to ground. For the deformed nuclei there does appear to be the same general dependence of these quantities, namely a systematic decrease from Ra and Th through the heaviest elements. For a plot of alpha reduced widths, see Fig. 1 of RASMUSSEN (1958). For plots of the odd-even mass differences, see Figs. 2 and 3 of NILSSON and PRIOR (1961). There are not enough data beyond $N = 152$ to determine whether the predicted minimum in Δ and reduced alpha decay rates exist.

The second factor, involvement of $\Omega = 1/2$ orbitals, should act in the same direction, the lighter deformed nuclei receiving heavier contributions from these favourable orbitals.

The third factor should operate in a contrary fashion, and in the overall dependence of reduced alpha transition probabilities the first two factors apparently dominate.

Acknowledgements

The major computational work was carried out on the IBM-709 computer of the Lawrence Radiation Laboratory, Berkeley, California, under the auspices of the U.S. Atomic Energy Commission. H. J. Mang wishes to acknowledge support of a Deutsche Forschungsgemeinschaft grant when this work was intitiated in Berkeley in 1959. J. O. Rasmussen expresses gratitude to Professor Aage Bohr for the hospitality of the Institute of Theoretical Physics, Copenhagen, in 1961–1962, and to the National Science Foundation for a Senior Postdoctoral Fellowship.

We give special thanks to Professor J. H. D. Jensen for his hospitality and financial assistance to J. O. Rasmussen during his two-week visit in Heidelberg. Likewise, we are grateful to Professor Aage Bohr for inviting and assisting H. J. Mang to make a two-week stay in Copenhagen to complete this paper.

V. G. SOLOVIEV (Physics Letters **1**, 202, 1962) has recently published some studies of the alpha-decay enhancement due to the superfluidity properties of nuclei, finding also a very large enhancement given to favoured decay. Soloviev found an enhancement factor of 1700 for the alpha decay of Cm^{244}. This factor is to be compared with our factor of 320 for Cm^{242} when the sum runs over ten proton and ten neutron orbitals; our factor would go roughly to $\sim$ 1300 for summation over all orbitals in three oscillator shells. It is not clear to us how many orbitals are included in Soloviev's summation and it is important to note that the wide fluctuation of our Γ_{00} entries in Table II calls for caution regarding Soloviev's assumption of constancy (his eq. (5)). In view of the differences in our calculations the enhancement factors of 1700 and $\sim$ 1300 would seem to be in satisfactory agreement.

Appendix

Coulomb Excitation Corrections

Consider equations governing the barrier transmission of alpha waves in the presence of a nuclear quadrupole potential

$$\frac{d^2 u_l}{d\varrho^2} - \left[\frac{2\eta}{\varrho} - 1 + l(l+1)\left(\frac{1}{\varrho^2} + \varepsilon\right)\right] u_l = \frac{q}{\varrho^3} \sum_{l'} \langle l' \mid P_2 \mid l \rangle u_{l'} \tag{A. 1}$$

and the effects of quadrupole coupling on the wave equation in the region near and outside the classical turning point. JACOBSOHN and MILLER (1959) have pointed out the connection between Coulomb excitation matrix elements and the imaginary components of the matrix transforming the alpha wave vector from the barrier region to the vector at infinity. Using this result and the symbols of ALDER *et al* (1956) we may write the matrix elements in lowest order as

$$\left.\begin{aligned} \hat{k}_{ll'} &= \delta_{ll'} - iq\, M_{ll'}^{-3} \langle l' \mid P_2 \mid l \rangle, \\ \text{where} \quad M_{ll'}^{-3} &= \int_0^\infty I_l(\eta_l \varrho)\, I_{l'}(\eta_l \varrho)\, \varrho^{-3}\, d\varrho, \quad \text{where} \quad \eta_l = \eta(1-\varepsilon)^{-1/2}. \end{aligned}\right\} \tag{A. 2}$$

Nosov's formula for the imaginary component, in these units, is equivalent to setting

$$M_{ll'}^{-3} = \frac{1}{6\eta^2} \tag{A. 3}$$

and this is just the limit of the radial integral for $\eta \gg l$ and $\varepsilon = 0$. The approximation is a fairly good one for the cases of practical interest in alpha decay.

A more general formula for all l but $\varepsilon = 0$ is (II. E. 75) of ALDER et al. (1956)

$$M_{ll+2}^{-3} = \frac{1}{6\,|\,l+1+i\eta\,|\,|\,l+2+i\eta\,|}\,. \tag{A. 4}$$

They give a somewhat more complicated formula for M_{ll}^{-3} which is not repeated here. Correction for $\varepsilon \neq 0$ can be made on the matrix element from the tables of the semi-classical Coulomb excitation integrals of ALDER et al. (1956).

The phase shift approximation method of CHASMAN and RASMUSSEN (1958) can be used to calculate the imaginary matrix elements and yields values exactly 3/2 that of Nosov (1957). The error arises from taking the interaction as a $\frac{1}{\varrho^2}$ instead of a $\frac{1}{\varrho^3}$ dependence.

For example, the $\hat{k}_{24}$ matrix element for Cm^{242} with $Q_0 = 10.96 \times 10^{-24}$ cm^2, $q = 320$, $\eta = 23.7$. $\varepsilon = 0.0011$ has an angular matrix element $6/7\sqrt{5}$, a radial factor (assuming $\varepsilon = 0$) of 0.093, a correction for finite ε of 0.87 for a value $\hat{k}_{24} = -0.031$ i. Nosov's formula yields a value about 15% too high. This matrix element should establish a lower limit on the ratio of intensities of $l = 4$ to $l = 2$ groups near Cm^{242}. That is

$$\frac{\text{Intensity}\,(l=4)}{\text{Intensity}\,(l=2)} \geq (0.031)^2 \frac{v_4}{v_2} = 9.5 \times 10^{-4},$$

where v_2 and v_4 are alpha velocities at infinity.

The experimental ratios in Cm^{242} and Cm^{244}, respectively, are 11.4×10^{-4} and 7.3×10^{-4}. Cm^{244} falls slightly below the limit, suggesting that the quadrupole moment of daughter Pu^{240} should be at least 15% lower than the 11 barns assumed or that the experimental intensity of the $l = 4$ group is in error on the low side.

H. J. Mang

Institute for Theoretical Physics
University of Heidelberg
Heidelberg, Germany.

J. O. Rasmussen

Institute for Theoretical Physics
University of Copenhagen
Copenhagen, Denmark.

On leave from Department of Chemistry and
Lawrence Radiation Laboratory, University of California,
Berkeley, California, U.S.A.

References

Alder, Bohr, Huus, Mottelson, and Winther (1956) Revs. Modern Phys. **28**, 432.
Belyaev, S. T. (1959) Mat. Fys. Medd. Dan. Vid. Selsk. **31**, No. 11.
Blomqvist, J. and Wahlborn, S. (1960) Arkiv för Fysik **16**, No. 46.
Bohr, A. and Mottelson, B. R. (1953) Mat. Fys. Medd. Dan. Vid. Selsk. **27**, No. 16.
Brussaard, P. J. and Tolhoek, H. A. (1958) Physica **24**, 263.
Casimir, H. (1934) Physica **1**, 193.
Chasman, R. and Rasmussen, J. O. (1958) Phys. Rev. **112**, 512.
Fröman, P. O. (1957) Mat. Fys. Skr. Dan. Vid. Selsk., **1**, No. 3.
Gol'din, L. L., Novikova, G. I., and Ter-Martirosyan, K. A. (1959) Zh. Eksp. i Teor. Fiz., **36**, 512., Soviet Physics JETP, **9**, 356.
Gol'din, L. L., Adel'son-Velskii, G. M., Birzgal, A. P., Piliia, A. D., and Ter-Martirosyan, K. A. (1958) Zh. Eksp. i. Teor. Fiz. **35**, 184, (1959), Sov. Phys. JETP **8**, 127.
Harada, K. (1961) Progr. Theor. Phys. (Japan) **26**, 667.
Herman, R. and Hofstadter, R. (1960) "High Energy Electron Scattering Tables", Stanford Press; Stanford, California.
Igo, G. J. (1959) Phys. Rev. **115**, 1665.
Jacobsohn, B. A. and Miller, L. W. (1959), Comptes Rendus du Congrès International de Physique Nucléaire, Paris 1958, p. 900 (Dunod, Paris 1959).
Kjällqvist, K. (1958) Nuclear Phys., **9**, 163.
Mang, H.-J. (1957) Zeits. f. Physik **148**, 582.
(1959) Sitzungsberichte der Heidelberger Akademie der Wissenschaften, 299.
(1959a) "Theory of Alpha Decay", Univ. of California. Radiation Laboratory Report 8931 (unpublished).
(1960) Phys. Rev. **119**, 1069.
Mang, H.-J. and Rasmussen, J. O. (1961) Proceedings of the 1961 Manchester Conference on Nuclear Structure.
Mottelson, B. R. and Nilsson, S. G. (1959) Mat. Fys. Skr. Dan. Vid. Selsk. **1**, No. 8.
Nilsson, S. G. (1955) Mat. Fys. Medd. Dan. Vid. Selsk., **29** No. 16.
Nilsson, S. G. and Prior, O. (1961) Mat. Fys. Medd. Dan. Vid. Selsk. **32**, No. 16.
Nosov, V. G. (1957) Dokl. Akad. Nauk, S.S.S.R., **112**, 414.
(1959) Zh. Eksp. i Teor. Fiz. **37**, 886, Soviet Physics JETP, **10**, 631 (1960).
Pennington, E. M. and Preston, M. A. (1958) Canad. J. Phys. **36**, 944.
Rasmussen, J. O. (1959) Phys. Rev. **113**, 1593.
Rasmussen, J. O. and Hansen, E. R. (1958) Phys. Rev. **109**, 1656.
Stephens, F. S., Asaro, F. A., and Perlman I. (1959) Phys. Rev. **113**, 212.
Strutinsky, V. M. (1957) Zh. Eksp. i Teor. Fiz. **32**, 1412, Soviet Physics JETP **5**, 1150.
Szymański, Z. (1961) Nuclear Physics **28**, 63.
Thomas, R. G. (1954) Progr. Theor. Phys. **12**, 253.
Woods, R. D., and Saxon, D. S. (1954) Phys. Rev. **95**, 577.
Wilkinson, D. H. (1961) Proceedings of the 1961 Manchester Conference on Nuclear Structure.
Zeh, H. D. and Mang, H. J. (1961) Nuclear Physics **29**, 529.

Indleveret til Selskabet den 28. februar 1962.
Færdig fra trykkeriet den 6. august 1962.

On direct application to the agent of the Academy, EJNAR MUNKSGAARD, Publishers, 6 Nörregade, Köbenhavn K., a subscription may be taken out for the series *Matematisk-fysiske Skrifter*. This subscription automatically includes the *Matematisk-fysiske Meddelelser* in 8vo as well, since the *Meddelelser* and the *Skrifter* differ only in size, not in subject matter. Papers with large formulae, tables, plates etc., will as a rule be published in the *Skrifter*, in 4to.

For subscribers or others who wish to receive only those publications which deal with a single group of subjects, a special arrangement may be made with the agent of the Academy to obtain the published papers included under one or more of the following heads: *Mathematics, Physics, Chemistry, Astronomy, Geology.*

In order to simplify library cataloguing and reference work, these publications will appear without any special designation as to subject. On the cover of each, however, there will appear a list of the most recent paper dealing with the same subject.

The last published numbers of *Matematisk-fysiske Skrifter* within the group of **Physics** are the following:

Vol. **1**, nos. 3, 6, 8–11. – Vol. **2**, nos. 2–3.

Printed in Denmark
Bianco Lunos Bogtrykkeri A/S

Det Kongelige Danske Videnskabernes Selskab

Matematisk-fysiske Skrifter

Mat. Fys. Skr. Dan. Vid. Selsk.

Bind **1** (kr. 141,00)

kr. ø.

1. Brodersen, Svend, and Langseth, A.: The Infrared Spectra of Benzene, sym-Benzene-d_3, and Benzene-d_6. 1956 14,00
2. Nörlund, N. E.: Sur les fonctions hypergéométriques d'ordre supérieur. 1956 .. 15,00
3. Fröman, Per Olof: Alpha Decay of Deformed Nuclei. 1957 20,00
4. Brodersen, Svend: A Simplified Procedure for Calculating the Complete Harmonic Potential Function of a Molecule from the Vibrational Frequencies. 1957 10,00
5. Brodersen, Svend, and Langseth, A.: A Complete Rule for the Vibrational Frequencies of Certain Isotopic Molecules. 1958 6,00
6. Källén, G., and Wightman, A.: The Analytic Properties of the Vacuum Expectation Value of a Product of three Scalar Local Fields. 1958 15,00
7. Brodersen, Svend, and Langseth, A.: The Fundamental Frequencies of all the Deuterated Benzenes. Application of the Complete Isotopic Rule to New Experimental Data. 1959 10,00
8. Mottelson, Ben R., and Nilsson, Sven Gösta: The Intrinsic States of Odd-A Nuclei having Ellipsoidal Equilibrium Shape. 1959 22,00
9. Källén, G., and Wilhelmsson, H.: Generalized Singular Functions. 1959 6,00
10. Møller, C.: Conservation Laws and Absolute Parallelism in General Relativity. 1961 15,00
11. Soloviev, V. G.: Effect of Pairing Correlation on Energies and β-Transition Probabilities in Deformed Nuclei. 1961 8,00

Bind **2**

(*uafsluttet/in preparation*)

1. Higgins, Joseph: Theory of Irreversible Processes. I. Parameters of Smallness. 1962 17,00
2. Gallagher, C. J., Jr., and Soloviev, V. G.: Two-Quasi-Particle States in Even-Mass Nuclei with Deformed Equilibrium Shape. 1962 18,00
3. Mang, H. J., and Rasmussen, J. O.: Shell Model Calculations of Alpha Decay Rates of Even-Even Spheroidal Nuclei. 1962 12,00
